

Go-Smart: Open-Ended, Web-Based Modelling of Minimally Invasive Cancer Treatments via a Clinical Domain Approach

Phil Weir ¹, Roland Ellerweg ², Stephen Payne ³, Dominic Reuter ², Tuomas Alhonnoro ⁴, Philip Voglreiter ⁵, Panchatcharam Mariappan ¹, Mika Pollari ⁴, Chang Sub Park ³, Peter Voigt ⁶, Tim van Oostenbrugge ⁷, Sebastian Fischer ⁸, Peter Kalmar ⁹, Jurgen Futterer ⁷, Philipp Stiegler ⁸, Stephan Zangos ⁹, Ronan Flanagan ¹, Michael Moche ⁶, and Marina Kolesnik ²

¹NUMA Engineering Services Ltd.,

²Fraunhofer Institute for Applied Information Technology,

³University of Oxford,

⁴Aalto University,

⁵Technical University of Graz,

⁶Leipzig University,

⁷Radboud University Clinic Nijmegen,

⁸University Hospital Frankfurt,

⁹Medical University of Graz

Abstract

Clinicians benefit from online treatment planning systems, through off-site accessibility, data sharing and professional interaction. As well as enhancing clinical value, incorporation of simulation tools affords innovative avenues for open-ended, multi-disciplinary research collaboration. An extensible system for clinicians, technicians, manufacturers and researchers to build on a simulation framework is presented. This is achieved using a domain model that relates entities from theoretical, engineering and clinical domains, allowing algorithmic generation of simulation configuration for several open source solvers.

The platform is applied to Minimally Invasive Cancer Treatments (MICTs), allowing interventional radiologists to upload patient data, segment patient images and validate simulated treatments of radiofrequency ablation, cryoablation, microwave ablation and irreversible electroporation. A traditional radiology software layout is provided in-browser for clinical use, with simple, guided simulation, primarily for training and

research. Developers and manufacturers access a web-based system to manage their own simulation components (equipment, numerical models and clinical protocols) and related parameters.

This system is tested by interventional radiologists at four centres, using pseudonymized patient data, as part of the Go-Smart Project (<http://gosmart-project.eu>). The simulation technology is released as a set of open source components (<http://github.com/go-smart>).

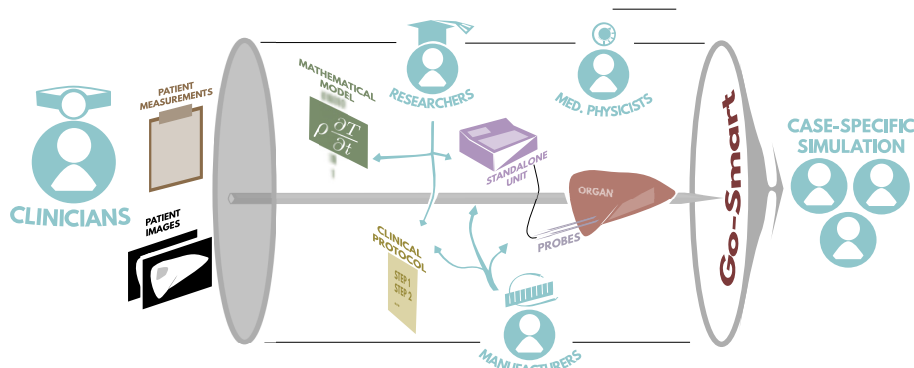


Figure 1: Graphical abstract

1 Introduction

Computer simulation technology can benefit clinicians and patients through training, education and planning [45]. For greatest effect, however, direct co-operation between clinicians, engineers and computational scientists is required [45]. This paper presents a system of pre-packaged ancillary tools, including a web-based radiological interface, image manipulation and a simulation architecture. Such an approach reduces the required collaboration skill-set to those directly relevant to the research or training at hand, and can remove web development as a limiting factor in web-based clinical training, commercial product development and simulation research.

In surgical training, acquisition of basic skills is moving from the operating theatre to educational settings, building an increasing need for testable, extensible educational surgical software. Moreover, experienced clinicians must gain experience using new technology as it is introduced, another important application of computational and non-computational simulation [20]. In general, predicting the outcome of minimally invasive therapies, particularly those involving thermal ablation, remains challenging due to the many factors influencing the procedure. Providing a platform for such training in a specific discipline requires engagement of both junior and senior clinicians for these reasons.

Manufacturers must also be involved: their consideration of clinicians' needs is crucial, and includes areas potentially outside core competencies, such as

software user experience [69]. This can create a significant cost and personnel burden in a green-field project. Reduction of newly designed interfaces can help avoid unpredicted challenges, benefiting from both user familiarity and a history of integrated feedback. By engaging with established tools, manufacturers gain insights into clinician and researcher behaviour at a preliminary stage, prior to costly investment in a software development or support infrastructure. Structured engagement of manufacturers with practitioners in simulated settings is encouraged [69].

The translational link between researchers and clinicians is also an essential element to support: the existence of a marked gap between research outcomes and implementation is well-established [27]. Encouraging awareness of developing best practice and technical evolution is therefore an important role of those engaged in establishing it [27]. Within clinical research itself, the need for research-relevant information systems has been identified as one of a number of research challenges, as are infrastructure investment and training. Public participation, also, is essential and can be impeded by lack of standardization and conflicts of interest. Together, these emphasize the need for vendor-independent, research-supporting IT frameworks, complementing clinical skill-sets and facilitating effective interaction between the worlds of research and practice [76].

The importance of effective and well-documented clinical trials is emphasized by another professional communication gap - that between trial outcomes and other forms of predictive study. Such discrepancies may arise from publication bias, inaccessibility of animal study registers and methodological limitations, amongst other factors [59]. A closer loop must be established between clinical trialists and experimentalists to ensure shortcomings in preliminary research are identified and resolved [59]. Providing a simplified, standardized and accessible online interface reduces the practical costs and obstacles to setting up a clinical or pre-clinical trial, and to the cataloguing and sharing of trial results.

In contrast to offline, non-web-based systems, an online web-based interface allows users in different institutions to interact on the same system, and, in particular, clinicians to use parameters and models dynamically defined by manufacturers and researchers. It also allows users to access data on their own devices off-site, for example, when meeting. This is practical only with a web-based system.

The project discussed in this work, the Go-Smart project [82], provides a web platform for highly adaptable simulation of minimally invasive cancer treatments. This avoids a computational system that represents a frozen point of development, allowing new equipment, clinical protocols and numerical models to be incorporated.

Underpinning this functionality is a domain model relating interventional room practice, manufacturer equipment and numerical analysis. It provides a framework for defining allowable combinations of entities, with a hierarchy of simulation parameters contributed by each. This is exported as a single, condensed configuration file for the simulation server. Results are viewed through an interactive, radiology-style web interface and may be validated against a segmented lesion, if available.

Clinicians interact with the system via a simple point-and-click interface in the web-site, when launching a simulation through the radiological patient management system. Entities may indicate certain parameters to be clinician-specifiable (e.g. duration of optional intervention steps, needle location), and the clinician is presented with a dynamically generated web-form. Technical users may access an additional interface, providing lower-level control of the parameters and properties of their contributed entities.

1.1 Novelty

This system is novel in several key respects:

- the approach to modelling general medical simulation problems, both
 - technically, by combining clinician-input data with researchers' sandboxed, uploaded computer code and parameters, through the Glossia system, described below, and
 - conceptually, through the Clinical Domain Model, described below, which structures this approach.

Together these allow a far greater depth of interaction between researchers, manufacturers and clinicians on a single platform than previously possible;

- 2D and 3D web visualization techniques, enabling a highly-responsive, easy-to-use, web-based radiology platform, comparable to offline systems, required for real-world clinician engagement;
- expansion and tuning of web-based image segmentation and registration techniques to ensure consistent and reliable processing of organ-level geometry, required for real-world clinician engagement;
- building a range of existing, and novel, numerical models surrounding a single medical application - Minimally Invasive Cancer Treatment (MICT) - and demonstrating the effectiveness of this system, taking individual patient datasets uploaded and segmented by clinicians through to simulation, and quantified model verification.

The Minimally Invasive Cancer Treatment simulation within the Go-Smart project is dependent on the innovations above, and the results that particular system can demonstrate have been shown by project authors.

However, the underlying technical and conceptual approach, applicable to general clinical problems, is first described in detail here. Its outcomes in the MICT application are shown to demonstrate this system's effectiveness in enabling highly-effective, clinician-driven use of dynamically-defined simulation.

In the paper, we show a novel architecture that makes online collaboration between researchers, manufacturers and clinicians possible, without the modelling restrictions placed on researchers by existing systems.

1.2 Application

The specific application under consideration is the web-based analysis of Minimally Invasive Cancer Treatments (MICTs). MICTs, in the scope of the project, comprise a set of methods for percutaneous tumor ablations under image guidance. In this context, we have developed a workflow across a consortium of nine partners, four clinical and five technical, that has been tested using incoming patient data over several years. In addition, we have been supported in our testing by input and feedback from external clinical users, MICT treatment manufacturers and, as the framework design approach is intended to be more broadly applicable, external biophysics researchers operating outside the MICT domain.

MICTs are a growing set of techniques for ablating cancerous tumours without the need for full surgical resection or when there are no surgical options. Such techniques include radiofrequency ablation (RFA), microwave ablation (MWA), cryoablation and irreversible electroporation (IRE), all of which are performed using percutaneous needles. The specific mechanisms of action, and underlying physics, are described in §3. As many of these techniques are becoming established and new approaches are continually appearing, it is challenging for interventional radiologists to gain and maintain familiarity with the available equipment and indications. Nonetheless, clinicians must remain aware of the changing field to provide optimal patient care - in RFA, experience has been shown to be correlated to treatment outcomes [31]. Moreover, they must be experienced in MICT selection and able to simulate or practice with new tools prior to clinical use. While modality-specific planning tools exist (e.g. [62, 38]), previously, there has been no effective tool for interventional radiologists (IRs) to predict patient-specific outcomes of a treatment, allowing for various modalities and equipment of various manufacturers.

This is a clinician-driven requirement to allow patient-specific comparison of approaches to treating a given tumour across multiple treatment modalities, as comparison within a single modality is an artificial constraint to finding an optimal treatment option.

The Go-Smart project seeks to rectify this, by providing a platform for clinicians to upload patient data, including CT and MRI images, then to plan, compare and validate treatment options. For a complete, ergonomic environment to be achieved, significant development has been undertaken: this encompasses image segmentation, image registration, simulation, modelling and visualization, brought together within a purpose-built scalable web framework. Validation data, for quantifying the performance of the segmentation, registration, modelling and simulation aspects, has been provided and reviewed by a series of clinical partners.

A core feature of the Go-Smart framework is its extensibility. To maintain pace with the state of the art going forward, additional mathematical models, simulation codes, equipment and even modalities may be added through the web interface, by independent researchers, technicians and manufacturers.

It is expected that the Go-Smart environment will provide a tool for indepen-

dent evaluation of equipment, training of clinicians, collaboration on treatment planning and medical research.

Even within existing MICTs, clinician experience is a highly determining factor for patient outcomes. Boundaries of tissue necrosis are hard to predict heuristically and medical simulation can help reduce patient exposure to outcomes that are difficult to predict based on clinical experience only. However, a single platform representing a snapshot of technical development in a rapidly changing field would quickly lose its relevance, and so the ability to incorporate new technologies through the web interface is indispensable to this aim.

1.3 Background

In the early 2000s, distributed computing projects began to appear in European health-care research: NeuroGrid [25], MammoGrid [5] and GEMSS [14], for instance, all began around this time. Applying principles of distributed computing in this sphere provided effective use of computational resources between institutions and opportunities for international collaboration. Complementing standalone tools that provide medical image and/or simulation analysis toolchains, such as SimBio [22], COPHIT [10], BloodSim [58], euHeart [73], IMPACT [57], or, much earlier, RAPT, newer platforms exist to bring analysis to a distributed setting, in some cases adapting existing standalone frameworks [13, 72]. The extension to a generic toolchain using scientific middleware is a challenge that has been impeded by closed extensions in proprietary tools [72], and evolutionary developments have moved closer to open, standardized protocols, incorporating web technologies for improved quality of service [21]. A more extensive overview of international computational projects in biomedicine is provided in [44] and [61].

Matching earlier distributed tools to a clinically usable web-based interface is an additional challenge, and one that has more recently been addressed with projects such as Aneurist [56] or neuGRID [61]. Simulation and patient-specific analysis algorithms may be later extensions to distributed data projects, as in the Health-e-Child and Sim-e-Child projects, respectively [23, 33, 51]. Other possible extensions include the expansion of user-facing web services [28] and broadened application of simulation tools through intercontinental amalgamation of data sources [75, 35]. Several such extensions may be seen in evolution between projects, adding significant value to existing tools [16].

Lessons learned from earlier distributed medical projects include the need for simple, widely-used standards, quality assurance, community building and good governance [80]. In particular, open infrastructure, specifically middleware, is a key component of successful projects [7, 6, 83, 3]. Adaptable open standards for defining simulation models, such as CellML, FieldML and SBML, are also important. However, they are not, in themselves, a panacea for providing modelling compatibility [36, 35, 50].

Many of these projects will be focused on medical research, rather than the clinical context. However, bridging the research-application gap within a platform provides opportunities to augment clinical decision making with pre-

dictive analysis, support clinical trial management, provide access to accumulated knowledge and, potentially, enhance patient-clinician communication [63]. Web-based services may even allow upload and analysis of data from home-monitoring systems, simultaneously providing a platform for patient support, clinician review and computational analysis [37]. With external clinicians and patients involved in platform use, a need arises for effective end-user engagement through channels such as social media [67]. Ultimately, if such tools, especially predictive simulation tools, are intended to inform medical procedure, an acceptable clinical workflow incorporating the output analysis must be formed [79]. In the research setting, an aim of web-based workflow tools, such as Galaxy [26], is to enhance accessibility, reproducibility and transparency.

Simulation workflows can facilitate patient-specific predictive analysis, based on the patient's medical images and quantitative indicators [18]. Moreover, they allow for both analysis and training to be incorporated into a web platform [55, 42]. However, incorporating computational modelling into education requires clarity around validation, documentation, copyright, confidentiality, duration and processing demands [42]. Simulation workflows may be primarily dynamically defined [54] or written in a more imperative, scripted manner [17]. While software such as Apache Taverna [32] and Galaxy [26] may provide very flexible workflow definition toolkits, a need for toolkit interchangeability still exists [68]. However, an established pattern for a number of medical simulation applications is the interlinking of an online knowledge database to a toolchain joining pre-processing, model creation, numerical solution and post-processing [11].

Other considerations in recent projects include convenience (no installation required for end-users), transparency, lightweight components, scalability and maintainability [70]. Adaptability, facilitated through lightweight tooling and a tight developer-stakeholder loop, is essential to account for the inevitable changeability of requirements throughout a clinical computing project [30]. Where distributed biomedical projects had generally been grid-based, cloud infrastructure is increasingly supported, for example, in the CBRAIN and VPH-Share projects [70, 12]. In particular, this allows extension of existing grid projects to a broader audience [12]. Nonetheless, as cloud resources are often run by third-party infrastructure as a service (IaaS) providers, quantitative comparison of cost and performance must be undertaken [15]. Within the Go-Smart project, simulation tools are consequently designed to be flexible with respect to deployment context.

While many of the existing projects have used an administrator-determined or architect-determined workflow, web-based biomedical simulation design is a growing approach. This is facilitated by a growth of workflow management systems, which can provide a convenient ready-made back-end. Such systems include the early Discovery Net, one of the first such systems, Triana, Apache Taverna and Kepler [19]. While many such bioengineering, bioinformatics and biomedical workflow systems now exist, it is less common to see such systems with an integrated web-based interface for dynamic inclusion of third-party workflows. Certain projects have based extended existing workflow packages

to improve cloud functionality or user-friendly web support, such as the Tavaxy project [2], combining the Galaxy system with the Taverna suite, WorkWays providing a web gateway for Kepler [52], or GPFlow wrapping Microsoft BizTalk and Human Workflow Services in a user-friendly scientific web interface [65]. In an offline setting, the GIMIAS open source framework provides a set of offline analysis and visualization tools that may be used inconjunction with Taverna to build complete research workflows, or preliminary clinical workflows [47].

The CHIC project [74, 77] provides a general, web-based cancer multi-scale modelling tool. They provide strong support for model adaptation and flexible architecture, supported by Apache Taverna workflow management. Moreover, this project incorporates human intervention steps in model execution and support probabilistic variables. They define the concept of hypermodels, which may be created by expert users as a workflow combination of pre-defined hypomodels through the web-based interface. Clinicians may execute upload patient data and perform simulations through this interface. While this project forms an important counterpoint to Go-Smart, the focus in the latter project is towards integrating manufacturer use cases and basic research with clinical use, by allowing the underlying hypomodels themselves to be created and managed through the interface. The CHIC project builds on the broad adaptability of its toolchain, allowing individual installations to provide new features. In the Go-Smart case, the clinical domain model, described in §2.4, is used to provide an opinionated framework, centred around medical interventions, but facilitating the cooperative building of new simulation strategies in that context.

The VPH-Share project incorporates a number of disparate medical areas in its flagship workflows: @neurIST, euHeart, VPHOP and Virolab. Online, or offline, workflow composition is available through Taverna support [78]. Researchers may access a diverse range of components, and a strong cloud focus provides flexible capacity for computation and data storage [43]. Interactive workflow steps are enabled through launching interactive interfaces, such as GIMIAS, in a cloud-hosted virtual machine and providing web-based remote desktop access. This enhances existing desktop applications through web accessibility. Workflows may be developed through online tools such as OnlineHPC, or offline with Taverna. VPH-Share is focused on providing a very general platform supporting diverse research-driven workflows. In contrast, Go-Smart focuses on a radiologically-driven design, helping researchers bridge the discipline gap by adapting and extending the analysis workflow at a low level through scripting, or a high level through parameter adjustment and manipulation of conceptual clinical components (§2.4). This ensures a comfortable, familiar experience for clinicians, while maintaining flexibility and a low barrier for entry both to developers and high-level modellers.

Combining Go-Smart utilities with workflow management tools such as Taverna or OnlineHPC (<http://onlinehpc.com>), or a web-based research and data management tool such as VPH-Share, would provide useful future enhancements, integrating benefits of each project.

2 Methods

The Go-Smart distributed architecture is designed to ensure stability and scalability of the environment. Certain computationally intensive components have restrictive hardware or software requirements, so processing must be spread between multiple hosts. The architecture has been divided into distinct, independently-functioning components with real-time communication middleware linking physical machines. Clearly-defined interfaces describe input and output of each component and for the browser and VisApp clients.

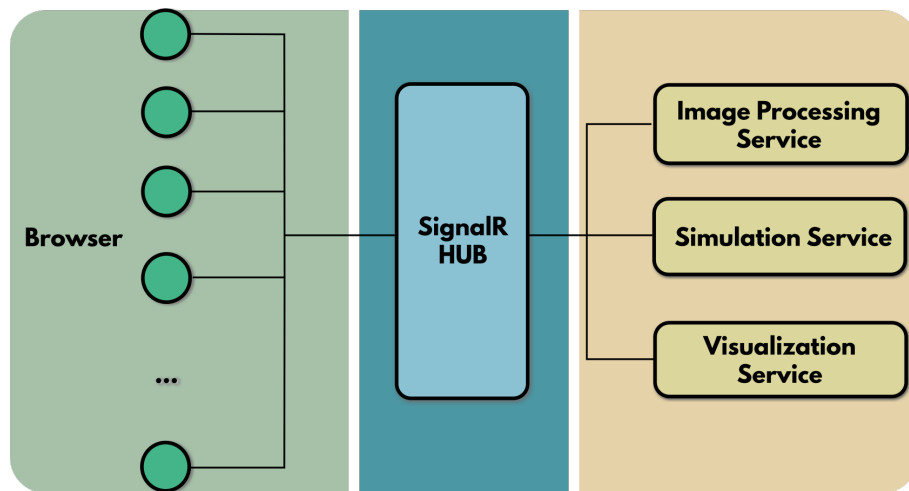


Figure 2: Overview of web application architecture. On the far left, various clients connect to the webserver running a SignalR Hub that, in turn, connects to simulation, segmentation and image processing services elsewhere within a privileged network. Business logic and views are provided by a standard ASP.NET MVC application hosted on the webserver.

The user roles discussed in §1 have highly contrasting requirements. Manufacturers want to add new equipment and algorithms easily. Radiologists want to use this equipment in a simulation environment, to familiarize themselves with a product, provide a training environment or to plan an intervention. Finally, researchers validate simulation results against laboratory tests or real-world clinical data, compare theoretical models, or experiment with protocol or equipment formulations.

To address these requirements, the following autonomous services have been implemented:

Image visualization server Due to the computational load of certain computational tasks required to support the radiological interface, a separate server handles these independently. This service processes the DICOM, segmentation and simulation data, generating axial, sagittal and coronal pictures which can be used in any common browser.

In particular, image re-slicing, allowing a user to adjust the axes along which the coronal, sagittal and axial views are defined, is a computationally demanding task to be completed with minimal interruption to the user experience during needle placement. Other tasks related to user-facing image generation and editing are implemented here, for example, contrast setting and editing of existing segmentations.

Image processing server This service segments structures such as organs, bronchi, vessel trees or tumours in the DICOM data provided by radiologists. This functionality is described in greater detail in §2.3.1.

Simulation server The simulation service uses the segmented structure and further information from parameters or needle positions to calculate a lesion. As a highly adaptable and flexible series of multi-process numerical workflows, the simulation framework is a distinct, re-usable concern, providing simple API endpoints for the web application via the Crossbar.io middleware. This functionality described in greater detail in §2.5.

On the client side, two complementary tools are available:

Browser client To use the Go-smart environment, the user needs only a normal web browser. Consequently, there are no special restrictions on the client machine. This is designed to provide interventional radiologists with a classic radiology workspace. Figure 3 shows this layout for segmentation [3(a)] and simulation [3(b)].

VisApp client When a clinician wishes to incorporate 3D interaction within the interface, they may use a specialized desktop application that wraps the website and injects a high-quality visualization widget into the fourth window, alongside the axial, sagittal and coronal views. Otherwise, the interface remains the same.

The services fulfill the basic functional requirements of the three user groups. For optimal user experience within the web environment, a good internet connection is required. In particular, the image visualization service must relay results in real-time, as it should respond efficiently to browser interactions, such as scrolling through a DICOM series, without visible latency.

The webserver system, hosting an ASP.NET application, marshalls communication between the client and server-side components. It is responsible for

handling transmission and caching of image data to ensure a favourable trade-off between data transfer and responsiveness. The application is designed to be scalable as usage increases. The Go-Smart database is also hosted on the web-server, which contains the anonymized patient data including medical images, 3D models and simulation results. To facilitate this, the open source ASP.NET SignalR library [1] connects services with the different browser sessions. SignalR uses HTML5 WebSockets to enable bi-directional communication between clients. If a client cannot use WebSockets, it falls back to other transport methods such as long-polling. Figure 2 shows the discussed components and the connections between them.

2.1 Information handling

2.1.1 Patient image data and pseudonymization

Image data is primarily captured in DICOM format, as the standard format for storing and processing data in medical imaging. The DICOM standard is an evolving standard, maintained by the DICOM Standards Committee. A comprehensive standard, it is formatted in 20 sections, covering over 4800 pages. Patient data in a DICOM file is stored with ‘tags’, which may be referred to using a tag name of the form (NNNN,MMMM) where NNNN and MMMM are four digit identifiers.

Within a DICOM series of images, no specific metadata file exists, nor a separate information database for the series. Instead, each image file contains a header with the metadata content ahead of the image data itself. Individual manufacturers of image acquisition systems will output DICOM files with private patient information often stored in non-standard tags.

The Go-Smart project involves four medical partners, who use a variety of equipment for different treatment modalities from different manufacturers. Medical image data has to be pseudonymized, with personally-identifiable references replaced by Unique Identifiers (UIDs), or anonymized before leaving the originating department. Mappings from UIDs to original cases are stored securely only at the originating department.

Prior to transfer to an image server, data must be pseudonymized. It is the responsibility of each department to properly perform this procedure before using patient data in the web interface. In order to provide a consistent approach, the following strategy is in place – all DICOM images used within the GoSmart project are pseudonymized by using an open source tool, *DICOM Browser* [8]. This tool has the capability to take a script file with commands for processing individual DICOM tags and built-in functions for the creation of new UIDs. A consortial agreement was established that only the following patient information should be preserved in the pseudonymized data: sex, age, date and time of the examination.

2.1.2 Ethics approval

IRB approval for data collection and processing within the project workflow was obtained by leading medical partner MUL under local reference AZ 206-13-15072013.

2.1.3 Case Report Forms

All relevant data from patient’s history – both image and clinical data – are documented within a comprehensive Case Report Form (CRF). This is available both as an offline document and integrated into the Go-Smart system, as part of its integrated patient record management. This document contains general patient statistics, such as age, sex, height and weight. The preoperative section of the CRF records characteristics of the target tumor such as size, qualitative perfusion and relevant pre-treatments, alongside pre-operative imaging notes and relevant blood parameters. During the MICT procedure, the exact course of the ablation is documented, especially technical parameters like energy deposition, number of needle positions, deviations from the protocol and what type of imaging was performed during the intervention. The post-operative section then evaluates details on follow up imaging, the size of the treatment lesion and once again relevant blood parameters.

The CRF can be supplemented by an appendix, which contains screenshots from key images like target tumor or other relevant imaging information. Furthermore, adverse events during the treatment must be recorded here.

The use of online CRFs also provides a useful MICT database for future collaborative research.

2.2 Usage

2.2.1 Primary user groups

Clinicians Once a clinician is logged onto the website, they may add a new patient record, capturing some or all of the wide variety of fields contained in standard Case Report Forms (§2.1.3). Pre-interventional CT and/or MRI images may be attached to the patient record and segmented using a semi-automatic process. Tailored segmentation tools are available for automatically identifying the lung, liver and kidney as potential ablation targets (additional organs may be added in future) and extracting a vessel tree from several contrast phases. With greater clinician involvement, other visible structures are segmented also, such as tumours and regions previously targeted by TACE.

Prior to performing a procedure, clinicians may place virtual percutaneous, needle-like probes in the segmented image, indicating the planned ablation target (Figure 3(a)). They set relevant configuration parameters, perhaps specific to a certain manufacturer or equipment model, and define an intended treatment protocol. At this point, a clinician may execute a simulation, which will show the approximate lesion created by such a treatment (Figure 3(b)). In most cases, this unattended simulation process takes 10-60 minutes, although shorter

or longer computations occur for certain combinations of protocol, equipment and modality.

After performing the procedure, clinicians may upload intra-operative images. These are then registered to the pre-operative data, which may be produced by distinct imaging modalities (CT to MRI and vice versa). This allows the clinician to identify the actual, rather than virtual, location of the ablation probes in the intra-operative image and so improve the simulation result.

The simulation models are tuned, by default, to predict the ablation lesion visible four weeks after the procedure. At this time, the clinician may wish to upload a set of post-operative images. The actual ablation lesion may be segmented from this image semi-automatically and, by registration with the pre-operative image, compared to the predicted outcome. A tool is provided to quantify the match.

Researchers, developers and manufacturers For users who wish to expand the Go-Smart framework, additional workflows are available. While much of the testing may be done using a workflow similar to that of a clinician, a technician may use the so-called *Developer Corner* to add a new mathematical model or piece of equipment.

Numerical models, needles, power generators, organs (contexts) and clinical protocols all have their own parameters, which may be adjusted through this interface. Technicians create their own version of a particular piece of equipment and simulate using their adjusted parameters, or test new theoretical models or modalities by defining tailored Elmer (finite element solver) SIF files [66] through the Developer Corner. Support for OpenFOAM [34] and Python, including the FEniCS libraries [49] has also been integrated. Due to the loosely-linked *Clinician Domain Model* (§2.4), re-use of existing or new numerical models and equipment is simple, allowing a technician to test a new theoretical model against a range of manufacturers probes, or vice versa.

2.2.2 Protocols

For each treatment modality, a tightly or loosely supplied recommendation by the manufacturer guides clinicians in the execution of the procedure. For RFA, this is often a complex algorithm, progressing through a series of possibly repeating steps according to the electrical impedance or average observed temperature shown on the power generator. For MWA, this is a much freer decision and clinicians choose a series of powers and durations to perform in sequence for each location. In cryoablation, rather than power, flow-rate is varied at set times for each probe. In IRE, probes are set, pairwise, to be anodes and cathodes with a sequence of potential differences applied between them. Within all of these protocols a degree of latitude is applied, based on clinical experience.

As such, the framework maintains a concept of a *protocol*, generally defined by a technician in Elmer’s MATC language [64]. This is normally a feedback loop that relates certain simulation variables to varying power, or another controlled variable, over time. These protocols often define the end of the procedure.

To allow straightforward use and customization by clinicians, these protocols may include parameters set at simulation time, through the user interface, and may indicate default widgets for clinician interaction (e.g. interactive power-time-graph).

2.2.3 Result Analysis

A separate validation component in the interface allows clinicians and technicians to view the registered, segmented ablation lesion in the same interactive pre-operative image viewer as the simulated ablation lesion. Using the methodology described in §4, a series of comparative statistics are calculated and presented.

2.3 Application components

2.3.1 Image segmentation and registration

This component allows a patient-specific 3D model to be built for clinician analysis and simulation, using CT and MRI images, based on a software library developed during the project. Separate relevant entities, such as organ, vessels, tumours and observed lesion are identified semi-automatically, with clinical support and adjustment through the radiological interface.

The target organ may be segmented fully automatically through organ-specific tools. This is achieved through a rough decomposition of abdominal structures into semantic objects and morphology-based segmentation.

For cases where fully automatic segmentation is not possible, a series of ‘drawing’ tools are provided – these include polygonal, slice-based inclusion or exclusion of regions; single-click, seed-point segmentation, identifying contiguous areas; and a free-hand painting tool.

Inner tubular structures, such as vessels, bile ducts and bronchi, are extracted by an altering Hessian-vessel model based segmentation method [4]. To provide data for segmenting vessel structures, a series of images must be obtained at separate phases of contrast enhancement – arterial, portal and venous. Segmented structures within these consecutive images are matched using image registration algorithms, and mapped into a single frame of references.

Similar techniques are used to match image data from pre-interventional acquisitions to that of peri-interventional and post-interventional acquisitions, with users identifying a series of corresponding landmark points in each image. Pre-interventional to post-interventional registration allows validation of ablation regions, between simulated and clinician-segmented profiles, as well as the inclusion of needle positions segmented from intra-operative imaging in the pre-interventional reference frame, for simulation.

2.3.2 Visualization

Using the Go-Smart web page in a browser allows a user to visually inspect all data generated during the workflow in a 2D, slice-based representation. A

standard radiological workstation is provided, encompassing sagittal, coronal and axial viewers. Within this interface are tools familiar to radiologists, such as image contrast windowing. Outline profiles of segmentation results, simulated ablation lesions and percutaneous needles are displayed within these views.

In addition to this radiological interface, a seamlessly integrated 3D visualization tool, named VisApp, is available for Microsoft Windows platforms. It exploits the local computing power of the client PC and minimizes delays between interaction and response. The application is implemented as an augmented web browser that identifies a hook on the Go-Smart web-page, and replaces the corresponding area with a render widget drawing from local GPU resources. This appears alongside the axial, sagittal and coronal image windows, providing a fourth window. This view is interactive and, using the SignalR pathways described in §2, causes the rest of the web-based interface to be updated in real-time, in response to user actions in the VisApp window and vice versa.

Advanced 3D volume rendering techniques are employed, which can adapt to the specifications of the local hardware. From basic direct volume ray casting [48], through advanced algorithms with optimal resource exploitation [81], to high-end global illumination techniques [40], a variety of options are supplied to the end-user, based on the capacity of the client machine (Figure 4). Both volumetric data and surface-based representations of segmented and simulated results, as well as needle models, are visualized through this interface. This allows user to explore treatment possibilities and evaluate validation data in 3D, as a supplement to traditional slice-based techniques.

2.4 Clinical domain model

2.4.1 Outline

This concept allows a database-persisted set of entities to collectively define a simulation strategy. The approach taken is more opinionated than existing model definition approaches (e.g. CellML, FieldML, SGML), in that it admits only certain, generic types of structure and entity, but allows for the model definition itself to be an arbitrary parameterized payload. As such, the clinical domain approach allows us to wrap CellML, say, as a numerical model taking parameters supplied by one or more clinical domain entities.

The fundamental abstract entities are:

- *Context**: environmental parameter set, such as per-organ default volumetric constants
- *Power Generator**: or any one-per-procedure parameter set. In the MICT context, a power generator, regulator or other standalone governing machinery. Generally dynamically defined by a manufacturer
- *Needle**: or any multiple-per-procedure parameter set. In the MICT context, generally a specific manufacturer-model of a percutaneous needle. Generally dynamically defined by a manufacturer

- *Protocol*: a set of algorithms mapping intraprocedural variables to model inputs. In the MICT context, generally a clinical protocol for indicating recommended clinician interaction with the apparatus as the intervention proceeds. Generally dynamically defined by a manufacturer or clinical researcher
- *Algorithm**: a single function definition, with text body, that may be interpreted by a particular simulation tool as mapping simulation-time inputs to quantitative outputs. In the MICT context, a specific output algorithm for a clinical protocol, giving, for instance, adjusted power or protocol phase number. Generally dynamically defined by a manufacturer or clinical researcher
- *Numerical Model**: parameterized definition of numerical model or settings for simulation software. In the MICT context, a parameterized Elmer (or other FE/FV solver) simulation definition. Generally dynamically defined by a medical physicist or biophysical researcher
- *Combination*: valid, simulatable set of the above entities. Generally dynamically defined by a manufacturer or biophysical researcher
- *Modality*: grouping of above entities, except Context, indicating a type of treatment. In the MICT context, this is RFA, MWA, Cryoablation, IRE (or other simulatable treatment)
- *Parameter*: uniquely-named, reusable token representing an item of information, possibly with a default value, type and/or entry widget. Parameter names are generally in capitalized snake case (underscore-separated) for flexibility and ease of identification. This appears as, for example, CONSTANT.INPUT.POWER.
- *Parameter Attribution*: a specific application of a Parameter to one or more of the starred entities, possibly with overriding value, type and/or entry widget
- *Argument*: a simulatable, intraprocedural output of the intervention, such as time or, where appropriate, power, clinical protocol phase, temperature observed by apparatus, etc.
- *Result*: a simulatable output of the procedure

The relationship between these entities is depicted in Figure 5. In addition to the Combination and Parameter Attribution relationships noted above, a many-to-many relationship can specify physically valid linkages of Power Generator and Needle. This helps a manufacturer to sensibly constrain the possible Combinations that may later be added by a clinical researcher or other downstream user.

These entities are stratified into several layers representing abstract entities, simulation-time entities and case-specific entities (Figure 6). Certain of these

entities are related through concretization or measurement, that is, such entities are derived from abstract forms supplemented by additional information, such as processed image data or clinician-selected options.

A natural progression may be seen between each tier. Abstract entities are defined by researchers and manufacturers. Through interaction with the radiology-style web interface and guided parameter entry, clinicians (or other users) create a set of simulation entities. This provides a complete set of data necessary for executing a simulation. Many simulations may be run by various users against a single Combination – a set of abstract definitions representing a procedure – each simulation creating a new set of Simulation entities.

For instance, an abstract needle may have a manufacturer model number and a range of settings. However, until it is *concretized*, that is, used in a simulation or actual intervention, it does not have a spatial position or a given number of separately configured needles. A Combination may have several possible needle model numbers that may be used. Each abstract needle will represent a different manufacture model. The distinction may be considered analogous to classes and objects.

A Simulation may have only one of those needle model numbers used several times, as separate Concrete Needles inheriting from a single Abstract Needle but each with separate tip and entry locations. Similarly, a Simulation may have any other repeated selection from the needle types allowed by the Combination. In the Power Generator – Needle cross-over table, a manufacturer may specify the minimum and maximum number of needles that may be used with a single generator, and so for a given simulation using that Power Generator. In a more general sense, this provides a separate relationship limiting the allowed combinations of one-per-simulation entity and multiple-per-simulation entities.

The third tier represents a set of physical facts relating to the specific intervention and/or patient, such as patient-specific measurements, image analysis and intervention outcomes. Some of this data may be used to create a Simulation, such as the segmented surfaces, or to validate it, such as measured outcomes.

2.4.2 Interaction of entities and workflow

An example workflow is presented showing the creation of entities defined above in normal practice. For simplicity, an example is chosen where the manufacturer defines exactly and only the equipment, a researcher prepares a protocol and numerical model, and a clinician runs a simulation based on their definitions.

Abstract Tier: Creating Combinations

Manufacturer When a manufacturer creates a Needle or Power Generator, a new entity in the Abstract tier is created. The manufacturer defines its characteristics through Parameters – these may be additionally constrained to vary by organ (Context), say, or when paired with an existing clinical protocol

(Protocol). In the case of a Needle, a geometric definition may also be provided. Parameter Attributions link equipment entities to each Parameter – if a Parameter does not exist with that name, one is created.

For each Parameter required, they may indicate whether a clinician can (or should) fill in a value, and what form widget to use, or whether a Combination including their equipment should only be definable if this Parameter has been given a value by another component of the Combination.

Researcher A researcher may add a numerical model to enable simulation of treatments. They prepare an entity-agnostic numerical model, for instance, using FEniCS and other scientific Python libraries. That is, it does not depend on the choice of Context, Needles, Power Generator or Protocols, but only on Parameters. They create a JSON file, declaring required Parameters and providing default values if appropriate. In Python, a helper module exists, which researchers may use to access Parameter and Region information (Example 1). When using the standard simulation workflows, for Elmer and FEniCS, researchers can assume a volumetric mesh has been provided in GMSH MSH format before their code runs, and all volumetric and boundary subdomains have known indices. The researcher may indicate required regions, with admissible multiplicities, in their model definition – these will be supplied by the output of the segmentation tool-chain.

Parameter values may be any JSON-representable type, although basic types provide most flexibility.

Example 1 Python snippet based on an IRE Numerical Model. *This converts the CGAL-supplied mesh to DOLFIN format and loads it. IRE electrode data is loaded from a Parameter and the mesh indices for vessel regions are extracted as integers. These may then be used for providing, e.g., boundary constraints and solving using FEniCS.*

```
from gosmart.parameters import P, R
import dolfin as d
import subprocess

subprocess.call([
    "dolfin-convert",
    "/shared/output/run/input.msh",
    destination_xml
])
mesh = d.Mesh(destination_xml)
electrode_triples = P.CONSTANT_IRE_NEEDLEPAIR_VOLTAGE
vessel_mesh_indices = [r.idx for r in R.group('vessels')]
```

In the Elmer case, using Jinja2-templated SIF files (<http://jinja.pocoo.org>), the syntax for Parameter access is similar.

For each Parameter required, a researcher may indicate whether a clinician can (or should) fill in a value, and what form widget to use, or whether a

Combination including their model should only be definable if this Parameter has been given a value by another component of the Combination.

Combination creation Either the researcher or manufacturer may add a new Combination, or set of Combinations, to make use of these models and equipment. All Simulations are based on an existing Combination.

Each Combination includes a single Numerical Model, Power Generator, Context, Protocol (which may be trivial, not supplying any algorithms) and one or more Needles. When a Combination is defined, the system confirms that all Parameters defined by a member of the Combination are either filled with default values, or allow values to be provided at simulation-time. Otherwise, it will refuse to create the Combination – this provides a crucial validation step, ensuring equipment and contexts, such as organs or phantoms, are pairable with the numerical models.

Simulation and Case Tiers: Using Combinations

Clinician A non-technical user, or technical user following their workflow, will upload patient data or experimental data. This creates certain Case Tier entities, such as defining a specific concrete context, indicating that this case is in a human liver, say, or an *ex vivo* muscle sample. The segmentation process identifies a series of regions with concrete geometric extents.

The user may then wish to run a Simulation. Only existing Combinations may be used for Simulation. The user picks a Power Generator and Clinical Protocol they wish to use via HTML drop-down boxes. None, one or more Needles (as permitted by the model) are added by the user via another drop-down box. The user identifies a tip location and organ entry-point for each by clicking in the radiology planes. These Concrete Needles, a series of Abstract Needles augmented with a specific geometric location, are saved.

Once the Needles are placed, only the Numerical Model remains a free selection. For each such selection, the administrator chooses one Combination to be marked *public*, to avoid non-technical users ever being confronted with a choice of Numerical Models. However, this public marker does not apply to technical users, and they are presented with a final drop-down menu of Numerical Models.

This process specifies the Combination completely, and the associated Parameters which have been marked for clinician input are presented in a user-friendly HTML form, alongside the radiology view. When they finally execute the Simulation, the Parameter values are saved as Concrete Parameters attached to the Simulation. They are no longer related to their source entity, except in the case of Needle Parameters, which are then tied to the Concrete Needles added above.

The Simulation definition is sent to the simulation orchestration tool via WAMP middleware. In the Go-Smart context, this is a transition from a .NET web application to one or more Linux back-end hosts.

2.5 Simulation orchestration

In creating a new simulation, the synthesis of members of a Combination into a single set of simulation settings is the responsibility of the web infrastructure, rather than the simulation orchestration tool. To enable clean exchange of model settings, without leakage of entity identities, a simple XML sublanguage has been defined: GSSA-XML. This contains only Simulation tier information necessary to execute a numerical analysis (i.e. that required by the Numerical Model entity). Its purpose is to prevent entity-specific behaviour on the simulation side, and ensure application-side entity extensibility independent of the simulation tool.

The orchestration tool that converts GSSA-XML into workflow-specific settings and launches individual simulation containers, is an open source package named Glossia, developed as part of Go-Smart. It hooks into the middleware by providing a series of WAMP end-points. While any WAMP router is adequate, a sample configuration is provided for the Crossbar.io software. This architecture enables a simulation to be executed and monitored from a process on any accessible machine in any language that has WAMP bindings. Glossia interaction has been tested from C#, Python, PHP and Javascript clients. The language of the workflow tools, inside the simulation container, is entirely independent of Glossia.

The Glossia server accepts a GSSA-XML simulation definition and examines it for a specific Numerical Model *family* – this is part of the Numerical Model’s entity definition. A family is defined to be a pair: a specific Docker image for performing numerics and a Python ‘mortar’ module, used to translate GSSA-XML into the necessary numerical package configuration. For Python-scripted simulation workflows, which can import the Glossia Python Container Module, no additional plug-in is required, making the creation of additional Docker families simpler. The developer may access all needles, parameters and computational regions through this module as normal Python structures, leaving communication detail to the Glossia tools.

For a given family, the configuration may be very general. In the case of the FEniCS [49] family, the configuration is a numerical Python module that may use any of a range of numerical Python libraries accessible inside the container, and possibly not the FEniCS library itself.

2.5.1 Docker simulation containers

The usage of Docker in non-scientific contexts has developed rapidly over the last two years. It provides lightweight, walled-off environments, with many of the benefits and few of the drawbacks of virtual machines. In particular, performance is similar to what may be seen without containerization. It is in production, providing user sandboxing for many Platform-as-a-Service (PaaS) providers. Its use in science and medicine is gradually being explored, as awareness of and experience in these technologies spreads from the web development and computer science.

As well as supporting a secure environment to run untrusted code, it allows reproducibility, ensuring that a researcher’s code will run on the Glossia server exactly as it does on the researcher’s personal workstation. To facilitate this, all Glossia tools are provided as open source software (<https://github.com/go-smart>), mostly under the Affero Gnu Public License (AGPL). Example families are included, wrapping the FEniCS and Elmer [66] numerical suites.

The AGPL requires a third party that wishes to provide a Go-Smart-like web service using Glossia to release any incorporated Glossia modifications, including addition of ‘mortar’ modules. However, the contents of new simulation container images or separate software on the host are not affected by this license and may be kept private (notwithstanding licensing restrictions of other software components). Libraries for use inside containers are provided under the MIT license, allowing proprietary or private code to be used for simulation if desired. The sale of more relaxed licensing is a potential component of project exploitation.

3 Theory of Minimally Invasive Cancer Treatments

The core mathematical models for simulating a series of ablation treatments are outlined. All are implemented, for the purposes of the web interface, using the Elmer framework, although some have purpose-written research implementations also in Python (FEniCS) or OpenFOAM. In most cases, the simulation process takes 10 - 60 min, unattended, for adequately refined results. However, as the environment permits on-going improvement and refinement of models, timing statistics are not fixed. While these models are based on established, published algorithms, additional project research has refined them and allowed identification of key patient-specific parameters [29].

3.1 Common Models of Thermal Modalities

Several of the modalities function by using hypo- or hyperthermia to destroy tissue. Two models, in particular, are thus shared:

3.1.1 Bioheat equation with perfusion term

As evidenced by analysis during the IMPACT project [39], [57], and following work of Kröger et al [46], a basic Pennes bioheat equation with added perfusion term is adequate to model first order effects of the thermal modalities. This formulation is used in a variety of numerical approaches to MICT modelling [9]. The governing equation is,

$$\rho c \partial_t T - k \nabla^2 T = Q_{\text{inst}} + Q_{\text{perf}},$$

where ρ , c , k and T are the density, specific heat capacity, heat conductivity and temperature of the perfused tissue, respectively. Q_{inst} represents the heat

flux due to the ablation instrument. The norming effect of tissue perfusion is defined to be,

$$Q_{\text{perf}}(x) = \begin{cases} \nu \rho_b c_b (T_{\text{body}} - T(x)) & \text{if } D(x) \geq D_0, \\ 0 & \text{otherwise} \end{cases}$$

with x being the spatial coordinate, $D(x)$ indicating the local fraction of cells considered dead and D_0 . The perfusion coefficient, ν is a material property of the local medium (e.g. lung tissue, liver tissue, tumour tissue), T_{body} is standard body temperature and T is the current local temperature. ρ_b and c_b represent the density and specific heat capacity of blood. Note that perfusion here is taken to be a field value, representing the thermal effect of blood-flow in vessels smaller than the imaging resolution.

3.1.2 Cell death model

While under hypothermia a simple empirical isotherm is used, for the case of hyperthermia, a more complex cell death model is used, developed during the IMPACT project [53]. Cells exist in one of three states: Alive, Vulnerable and Dead. Cells may transition from being Alive to being Vulnerable, from being Vulnerable to being Dead and from being Vulnerable to being Alive. The rates at which they do so are dependent on local temperature.

The fraction of cells at a location in an Alive, Vulnerable or Dead state is expressed in terms of A , V and D , respectively. Each variable lies between 0 and 1 and the sum of all three is consistently 1.0 – this allows the Vulnerability variable to be removed from the algorithm. The relationships are expressed as follows,

$$\begin{aligned} \frac{dA}{dt} &= -\bar{k}_f e^{T/T_k} (1-A)A + k_b (1-A-D), \\ \frac{dD}{dt} &= \bar{k}_f e^{T/T_k} (1-A)(1-A-D), \\ A|_{t=0} &= 0.99, D|_{t=0} = 0.0 \end{aligned}$$

The forward and backward rate coefficients, \bar{k}_f and \bar{k}_b may be constants or temperature dependent. By default, the lesion is estimated to be the region in which $D \geq D_0 := 0.8$.

3.2 MICT-Specific Models

3.2.1 Microwave ablation

This modality is modeled by coupling the above bioheat equation and death equation to a simplified Maxwell's Equations solver. The local value of Q_{inst} is calculated using a transverse-magnetic (TM) axisymmetric cylindrical solver. The primary equation is,

$$\nabla \times \left[\left(\epsilon_r - i \frac{\sigma}{\omega \epsilon_0} \right)^{-1} \nabla \times \mathbf{H} \right] - \mu_r k_0^2 \mathbf{H} = 0, \quad (1)$$

where ε_r and σ are temperature-dependent relative permittivity and conductivity of tissue, respectively, at the manufacturer’s stated frequency. z and r are the local cylindrical coordinates along the probe shaft and centred on its tip. k_0 and ω are the wave number in a vacuum and angular frequency, respectively. $\mathbf{H} = H_\phi \mathbf{e}_\phi$ is the magnetic field vector, approximated as having only an azimuthal component, H_ϕ . This may be used to calculate the local energy deposition into the tissue (SAR), through the relationship,

$$Q_{\text{inst}} = \frac{1}{2} \sigma |\nabla \mathbf{H}|. \quad (2)$$

As parameters in Equation 1 are temperature dependent, we can see the nonlinear coupling between the bioheat and coax equations. Unlike the simpler, linear model, without temperature dependent electromagnetic parameters, the nonlinear coupled problem tends to a steady-state solution over relatively short timescales. The steady-state magnetic field is obtained from the axisymmetric model with a fine resolution numerical mesh. This then supplies $\nabla \mathbf{H}$ for Equation 2, which may be used with temperature-varying σ in a time-stepping bioheat model. This enables microwave simulation to be performed in clinically applicable times.

The current model is based on the Amica Microsulis prototype probe, although on-going work is incorporating a second manufacturer’s configuration.

3.2.2 Cryoablation

While the basic model for this is the modified Pennes bioheat equation, a front-capturing multi-phase solver is used to ensure accurate representation of the change in physical properties due to the expanding ice ball. In particular, the numerical method used is the *effective heat capacity method*. Here, the latent heat of phase change is accounted for by an adjustment to the relationship between specific heat capacity and temperature. Moreover, a *mushy* region is admitted, permitting a smooth transition of physical properties. Mathematically, the effective heat capacity is given as,

$$c_{\text{eff}}(T) = \begin{cases} c_s, & T < T_s, \\ \frac{c_s + c_l}{2} + \frac{h_{\text{sf}}}{2(T_l - T_s)}, & T_s \leq T \leq T_l, \\ c_l, & T > T_l, \end{cases}$$

where h_{sf} is the latent heat of solidification, T is temperature, c is heat capacity and the subscripts l and s denote the *solidus* and *liquidus* states, respectively.

The thermal conductivity is then defined to be,

$$k_{\text{eff}}(T) = \begin{cases} k_s, & T < T_s, \\ k_s + \frac{1}{2(T_l - T_s)}(k_l - k_s)(T - T_s), & T_s \leq T \leq T_l, \\ k_l, & T > T_l, \end{cases}$$

where k is thermal conductivity. These effective values replace their equivalents in the Pennes bioheat equation and the resulting nonlinear equation is solved iteratively.

This model and protocol has been tested against ablations performed using Galil Medical Systems’ cryoablation technology.

3.2.3 Irreversible electroporation

IRE is modeled using a simple electric potential solver,

$$\begin{aligned}\nabla \cdot (\sigma \nabla \phi) &= 0, \\ \frac{\partial \phi}{\partial n} |_{A_i} &= V_i, \\ \frac{\partial \phi}{\partial n} |_{C_i} &= 0,\end{aligned}$$

with conductivity σ and electric potential ϕ . A_i and C_i are the i^{th} anode and cathode, respectively, and V_i is the defined potential difference between them.

Over the ordered sequence of pairings in the protocol, each of which is defined by two of up to six probes and their potential difference, the electrical properties change based on the deposited energy. The final lesion is defined as an isovolume based on a chosen threshold of the local energy maximum over the whole protocol sequence [60, 24]. Future work is required to determine precise parameters for heuristic thresholds.

3.2.4 Radiofrequency ablation

Rather than performing a Joule heating simulation for each execution of this modality, an empirical approach is generally used, consisting of a summation of Gaussian functions centred on suitably chosen points. This technique was validated during the IMPACT project, and avoids the extremely large meshes required to capture the < 1 mm diameter probe tines. Further studies using a calculated Joule heating field are planned. This model is tailored to the Angiodynamics RITA family of RFA needles, although extension work is ongoing to incorporate extensible-tine probes of another manufacturer.

The RFA power generator simulation accounts for the feedback loop based on the thermocouples at the tips of individual tines. Recommended clinical protocols may be followed automatically, where the simulation moves from one protocol step to the next based on temperature readings, for instance. Tines may be extended or retracted according to the protocol, and the input power is governed by a PID controller, with temperature as the primary variable (for RITA needles).

3.3 Extension

Mathematical models applied to other areas of the body or treatment methodologies may be integrated by creation of finite element configurations for already-incorporated simulation families, such as Elmer or FEniCS. As these families are modular, third party tools may be incorporated by the server administrator, as a separate Docker image, with preprocessing Python plug-in modules.

Numerical models built on top of this new family may be defined in any way parsable by the plug-in module and container image.

4 Results & Discussion

Sample results obtained using the Go-Smart workflow, demonstrating the effectiveness of the procedure, are presented. In keeping with the focus of the current work on simulation orchestration and model-building methodology, full validation studies examining the effectiveness of biophysical models of each MICT procedure will be the subject of future treatment-focused communications.

It should be reinforced that, within the context of this paper, our primary demonstration through these results is the effectiveness of the system for bringing together parameters, models and patient-specific data into representative simulated outputs. Full analysis and detailed validation of the models themselves is provided separately.

4.1 Evaluation measures

To provide evaluation of simulation performance, the ablation lesion as observed 4-6 months after the intervention is used as a reference. This is segmented by clinicians through the interface and may be registered into the same coordinate system as the pre-interventional segmentations, on which the simulation is based.

For demonstrating applicability to end-user workflows, comparison of size and shape is of primary interest. As organ-based registration between the pre- and post-interventional image acquisitions is affected by alterations in the relative locations of internal structures over the 4-6 week intervening period, a rigid-body registration is applied between the segmented and simulated ablation lesions. While this prevents us from measuring offset, it allows us to quantify shape and size deviation between the two ablation zones. Potential effects of this approach on measuring simulation accuracy are raised in the discussion of results.

The segmented ablation lesion volume, after rigid-body registration, is denoted S . The simulated ablation lesion volume is denoted Σ . Measures presented here are the *DICE* metric [DICE], *target overlap* or *sensitivity* [SN], *positive predictive value* [PPV] and *average absolute error* [AAE]. Measures used are established measures in image comparison ([41, 9]). These are defined as

follows:

$$\begin{aligned} \text{DICE} &= \frac{2|S \cap \Sigma|}{|S| + |\Sigma|}, \\ \text{SN} &= \frac{|S \cap \Sigma|}{|S|}, \\ \text{PPV} &= \frac{|S \cap \Sigma|}{|\Sigma|}, \\ \text{AAE} &= \int_{\partial S} \left\{ \inf_{\mathbf{y} \in \partial \Sigma} |\mathbf{x} - \mathbf{y}| \right\} d\mathbf{x} / |\partial S|. \end{aligned}$$

The DICE, SN and PPV values range from least match at 0.0 to identical overlap between S and Σ at 1.0. While the DICE value is symmetric, the SN and PPV together help indicate the dominant type of mismatch – false positive or false negative. The AAE value is an average of the minimum distance to a point on Σ from each point on S , and helps isolate surface comparison when considered alongside the volumetric measures. The mean, μ , and standard deviation, σ , of each measure is presented. The volumetric ratios are unitless. AAE is measured in millimetres. All values are rounded to 3d.p.

4.2 Radiofrequency ablation

	Organ	DICE	SN	PPV	AAE (mm)
RFA1	Liver	0.591	0.828	0.459	3.853
RFA2	Liver	0.711	0.818	0.628	3.393
RFA3	Liver	0.631	0.661	0.604	2.975
RFA4	Liver	0.657	0.503	0.946	2.957
RFA5	Liver	0.694	0.785	0.622	2.792
μ		0.657	0.719	0.652	3.194
σ		0.043	0.123	0.160	0.384

Table 1: Evaluation measures for a series of RFA treatments

All radiofrequency ablation interventions presented in Table 1 were performed at the Leipzig University Hospital [DE]. Through the web interface, clinicians at this institution uploaded patient image data, segmented and registered it, then prepared RFA simulations to match their treatment.

Cases RFA1-RFA5 do not generally show a larger SN value than PPV value or vice versa, suggesting that the simulated ablation zone is not systematically over- or under-estimating the segmented ablation zone size. The AAE is steady, 2.792 mm - 3.83 mm, indicating a fairly consistent shape deviation. Where the AAE is larger, the PPV is significantly lower than the SN, suggesting that these higher deviation cases are due to an overestimation of the true lesion size by the model.

The most and least severe deviations (as measured by AAE) are shown in Figure 7. In both cases, shape deviation can be seen between the registered segmented ablation lesion in purple and the simulated ablation lesion in organ. This similarity of shape deviation corresponds to the similar observed AAE values. The simulated RFA heat deposition profile is based on research outcomes of the IMPPACT project, and it is generally observed that segmented RFA lesions form approximations to this pattern. Both lesions were produced with Rita Starburst needles using a staged protocol, recommended by the manufacturer, intended to produce a 5cm-diameter lesion. The clinical steps and responses in this protocol are algorithmically defined in the Go-Smart database.

Not shown in Figure 7, to avoid obscuring the view of the ablation lesions, is the vessel tree. The effects of this structure may be seen to the far right of the simulated ablation in Figure 7(a), where the lesion profile curves inwards. The percutaneous needle is not shown - in both cases it lies approximately on the vertical axis, entering at the bottom of the figure and, in Figure 7(a), terminating inside the green tumour surface. The individual flexible tines of the Rita Starburst probe extend at separate stages of the protocol and lie a few millimetres inside the simulation extent shown.

In Figure 7(a), the clinically segmented lesion is shown prior to rigid-body transformation (in charcoal). The transformed version is shown in purple. The inaccuracy of the original 1-2 month follow-up registration may be seen by the offset of the tumour, which is segmented in the pre-interventional image, from the charcoal profile. In contrast, the base of the simulated lesion mostly covers the tumour. However, there may be a small local underestimation here, as no indication of under-treatment was given in the clinical report form (CRF). For clarity, only the transformed version is shown in most subsequent figures.

4.3 Microwave ablation

	Organ	DICE	SN	PPV	AAE (mm)
MWA1	Liver	0.503	0.349	0.903	3.682
MWA2	Lung	0.545	0.466	0.657	5.305
MWA3	Liver	0.722	0.579	0.958	2.285
MWA4	Liver	0.722	0.603	0.901	2.278
MWA5	Lung	0.650	0.517	0.870	4.071
μ		0.628	0.583	0.859	3.524
σ		0.090	0.091	0.104	1.15

Table 2: Evaluation measures for a series of MWA treatments

All microwave ablation interventions presented in Table 2 were performed at the Medical University of Graz [AU] (Liver) and University Hospital Frankfurt [DE] (Lung).

Cases MWA1-MWA5 generally have significantly larger PPV values than SV. All three cases performed in the liver have PPV values over 0.9, although

only two have DICE values over 0.7. The liver cases have a smaller AAE, with values between 2.2 mm and 3.7 mm, compared to the lung cases, with the AAE values of both being over 4.0 mm. This suggests that, both in the lung and in the liver, the MWA model may be consistently over-estimating the extent of the ablation lesion. The moderate AAE values in the liver suggest that there it is more accurately reflecting the shape than in the lung. Overall, the mean, μ , is similar to the RFA cases, but the standard deviation, σ , is much larger, approximately treble the presented RFA example.

In Figure 8, as in the RFA discussion, the two MWA cases with greatest and least AAE values, respectively, are shown. Alongside the vessel tree, an additional segmented structure is present in the lung simulations, the bronchi (not shown). In both images, it can be seen that the MWA profile forms an approximately obloid shape. While this is produced using bioheat transfer and a deposition profile derived from Maxwell’s electromagnetic equations, the simulated ablation region is similar in profile to descriptions in manufacturers’ literature.

The case with greater deviation, MWA2, is shown in Figure 8(a). The clinician-segmented tumour and ablation zone are significantly offset from the clinician-segmented needle. The simulation itself matches the needle location well and in one dimension, has similar extent to the segmented ablation lesion. However, in the directions perpendicular to the line of view, the segmented ablation has a much larger extent. In the second case, MWA4, shown in Figure 8(b), a much better match is visible. The tumour is mostly, but not entirely, covered by the simulation. The ablation extent in line with the needle is underestimated, however.

In the lung context, registration is considerably more challenging due to the large deformations in the medium, and this may contribute to the discrepancy observed in MWA2. In general, observed ablation profile deviations in the liver tend to be smaller. In addition, the MWA energy deposition profile is heavily dependent on the ablation probe’s internal geometry, thus the equipment model and manufacturer. While we have been able to produce models based on prototypal probe geometries, this specificity is believed to contribute to ablation underestimation in MWA4 and other liver and lung cases. A second manufacturer-specific geometry is under development.

4.4 Cryoablation

All cryoablation interventions presented in Table 3 were performed at the Radboud University Medical Centre [NE].

Performance in the CRYO1-CRYO5 cases is generally good, although no consistent pattern of under- or over-estimation is easily observable. The AAE values are generally low, although in CRYO1, all volumetric measures are below 0.74. CRYO5 has similar volumetric measures, but its AAE value is below 1.9, suggesting that deviation may be a relatively small offset. In CRYO3, an even lower AAE value is seen, but the SN value is the second lowest of the set, perhaps indicating that the segmented ablation in this case is uniformly larger

	Organ	DICE	SN	PPV	AAE (mm)
CRYO1	Kidney	0.619	0.553	0.739	2.905
CRYO2	Kidney	0.755	0.960	0.622	2.368
CRYO3	Kidney	0.796	0.682	0.955	1.591
CRYO4	Kidney	0.828	0.821	0.835	2.240
CRYO5	Kidney	0.743	0.748	0.739	1.859
μ		0.748	0.749	0.778	2.19
σ		0.071	0.142	0.111	0.450

Table 3: Evaluation measures for a series of cryoablation treatments

than the simulated profile.

As before, in Figure 9, the two cryoablation cases with greatest and least AAE values, respectively, are shown. While MWA and RFA are simulated using one needle embedded at a time, both cryoablation and IRE must cater for multiple needles simultaneously embedded in the computational mesh, as in Figure 9(b).

While the sizes are broadly similar, deviation is visible in CRYO1 both in shape and orientation. The tumour is not completely covered by either the segmented or simulated ablation, although there is a region of three-way overlap towards the base of the probe. Toward the tip, the probe itself leaves the organ, as well as the lesion regions - while heat transfer is simulated outside the organ in the cryoablation model, tissue necrosis is evaluated only inside the segmented organ region. All cryoablation cases considered using this tool are treatments of exophytic tumours and we see, both in CRYO1 and CRYO3, that the organ wall provides a limit for the segmented lesion. CRYO3 also shows needles exiting the lesions and organ, although the match between lesion extents is better.

The segmentation or registration may account for some of the difference between CRYO1 and CRYO3 accuracy, as we can see the segmented lesion follows the organ wall more accurately in the second case, but the simulation nevertheless underpredicts the breadth of tumour. While the proximity to the organ wall improves several aspects of the segmentation and registration process, it introduces additional complication into the modelling process, as the current model has little contextual information about the medium beyond the organ wall. Future evolutions may include additional segmented regions abutting the organ wall, allowing more accurate heat transfer modelling near the needle tip.

4.5 Irreversible electroporation

All irreversible electroporation interventions presented in Table 4 were performed at the Medical University of Leipzig [DE].

The IRE1-IRE5 cases show a variety in quality. The PPV values in cases IRE3 and IRE4 are very low, but more acceptable in other cases. The SN values are generally high with AAE inversely following the PPV, suggesting that the

	Organ	DICE	SN	PPV	AAE (mm)
IRE1	Liver	0.541	0.888	0.389	5.264
IRE2	Liver	0.588	0.859	0.447	3.944
IRE3	Liver	0.088	0.996	0.046	11.767
IRE4	Liver	0.086	0.944	0.045	13.024
IRE5	Liver	0.569	0.905	0.415	8.471
μ		0.374	0.917	0.268	8.48
σ		0.234	0.049	0.182	3.53

Table 4: Evaluation measures for a series of irreversible electroporation treatments

segmented ablation zones generally lie inside the simulated zones. The standard deviation in DICE and AAE, particularly, is much higher than in previous cases, suggesting that cases may be mixed between adequate prediction and inaccurate results.

In Figure 10, case IRE2 and case IRE4 are shown. In IRE2, we can see that for a small number of needles, close together, the cross-sectional size is similar, although the extent lateral to the needles is greater. In IRE4, the segmented ablation lesion lies mostly between the needles, intersecting only two. It covers little of the tumour, although no residual tumour tissue was identified in the follow-up acquisitions for this case. While the simulated ablation does cover the tumour and needles, it is considerably bigger than the segmented ablation.

In general, the IRE cases tend to match either acceptably well, or significantly over-estimate the observed lesion. In the latter cases, a segmented lesion disjoint from at least one needle is observed, an unlikely occurrence in the accepted physical theory, and consultation of the relevant medical images confirms that the segmentation matches the measured data. A possible explanation is that the necrotic tissue caused by the IRE ablation beings the healing process faster than in thermal modalities. This is supported by the absence of both tumour tissue and a visible ablation lesion across much of the original tumour extent. Preliminary work has taken place to compare simulated IRE lesions with lesion extents observed immediately post-intervention, rather than 1-2 months later, showing much more favourable comparison.

4.6 Project outcomes

The development of the Go-Smart tool gave rise to a number of key lessons that were learned and incorporated:

Microservices architecture To enable a scalable and resilient service, deployable locally or in the cloud, components must be cleanly articulated and re-usable.

Domain model spanning clinical and technical concerns To facilitate generic, open-ended simulation, relevant domain knowledge within the unified model must not be from a single sphere, but reflect both practical and theoretical modelling considerations.

Familiarity of interface For a system to be usable by interventional radiologists, the workflow must be a variation on standard interfaces. In particular, simulation definition must fit neatly within established tool layouts, and dynamically-added parameters should contain definitions for user-friendly widgets and labelling.

Status updating For longer, non-interactive steps, status updates should be provided, both for technical users to analyse progress and non-technical users to indicate continued processing. This necessitates a live, multi-step communications relay from the containerized simulation, through the simulation orchestrator, middleware and back to the client.

Broad clinical feedback is vital Having interventional radiologists using the system and analysing (pseudonymized) patient data within it is essential to provide insight for technical users into clinical issues with the system and to gather information on potential edge cases with patient imaging.

Interaction with manufacturers is needed to provide quality models Especially in multiphysics biomedical problems, manufacturer data and feedback is required to ensure modelling starts from an accurate basis.

In trials, patient-specific modelling requires on-going engagement between clinicians and modellers While Clinical Report Forms are the fundamental tool in contextualizing image data, there must be case-by-case discussion between clinicians and technical users to identify shortcomings in modelling, unpredicted issues and potential errors in parameter interpretation or measurement. In particular, an expertise gap between numericists' awareness of clinical received knowledge, and clinical understanding of biophysics modelling concerns, may only be adequately addressed by in-depth discussion of individual interventions.

5 Conclusions

This work has outlined a web-based platform, applied to image-guided Minimally Invasive Cancer Treatments, that serves the needs of clinicians, manufacturers and researchers simultaneously. To achieve this requires a conceptual model spanning the clinical and modelling concerns. For researchers, this multi-stage approach allows them to deploy new models or computational routines to the web-based platform with minimal additional burden. For manufacturers,

this provides a tool to demonstrate their products and increase awareness within the market. For clinicians, this provides a platform for training, collaboration and knowledge gathering.

The models used for Minimally Invasive Cancer Treatment were shown to be adequate for demonstration purposes and sufficiently varied to establish the necessary flexibility of the Go-Smart platform. Improvements, both in terms of speed and accuracy, may be made incrementally, and as a collaborative exercise through the web interface. At present, our models produce most favourable results for cryoablation, where bioheat transfer is the primary modelling challenge, and RFA, where a heuristic approach has been established. In microwave ablation, the sensitivity of the models to manufacturer-specific geometry and complexity of electromagnetic modelling remain a challenge. In IRE, the time-based definition of an ablation zone must be revisited.

Interaction between stakeholders of multiple groups is essential for development of reliable and, ultimately, clinically useful models. A process for facilitating this is required, and the refinements made during the Go-Smart project in response to user feedback have helped streamline it as an appropriate.

Producing a system that allows for extension of simulation capabilities by end-users of the web-interface has been achieved at a lower level than we have seen, although deployment of entirely new solver frameworks remains an administrative task. More generally, the cross-concern conceptual model and toolchain for containerized simulation orchestration is designed to be re-usable in other clinical application domains.

5.1 Future work

On-going trials with external technical groups are underway, within a MICT equipment manufacturer and a non-MICT-related biomedical research group. Alongside clinical feedback, this will provide us with a useful corpus of usability information to refine the current workflow.

To provide broader applicability, with low entry burden, existing open source medical simulation tools, such as SimTK [71], Chaste or OpenCMISS, may be pre-emptively incorporated as new Glossia families. In particular, wrapping Taverna or Galaxy as new families would allow much more complex workflows to be built, and be executable within our current architecture. Extending preliminary work (using Vigilant¹) to a more user-friendly set of web-based back-end tools, providing orchestration visualization and interactive log aggregation, will simplify management of simulation deployments in a cloud setting.

References

- [1] ASP .NET SignalR. Incredibly simple real-time web for .NET. *Www.signalr.net*.

¹<https://github.com/redbrain/vigilant>

- [2] Mohamed Abouelhoda, Shadi Alaa Issa , and Moustafa Ghanem. Tavaxy: Integrating Taverna and Galaxy workflows with cloud computing support. *BMC bioinformatics*, 13(1):1, 2012.
- [3] John Ainsworth. The challenges of clinical e-Science: Lessons learned from PsyGRID. In *Proceedings of the UK e-Science All Hands Meeting 2007, Nottingham, UK, September 10-13*. Citeseer, 2007.
- [4] Tuomas Alhonnoro, Mika Pollari, Mikko Lilja, Ronan Flanagan, Bernhard Kainz, Judith Muehl, Ursula Mayrhauser, Horst Portugaller, Philipp Stiegler , and Karlheinz Tscheliessnigg. Vessel segmentation for ablation treatment planning and simulation. In *Medical Image Computing and Computer-Assisted Intervention–MICCAI 2010*, pages 45–52. Springer, 2010.
- [5] S Amendolia, Michael Brady, Richard McClatchey , and Miguel Mulet-Parada. MammoGrid: large-scale distributed mammogram analysis. 2003.
- [6] S Roberto Amendolia, Florida Estrella, Chiara Del Frate, Jose Galvez, Wasseem Hassan, Tamas Hauer, David Manset, Richard McClatchey, Mohammed Odeh, Dmitry Rogulin et al. Deployment of a grid-based medical imaging application. *Studies in health technology and informatics*, 112:59–69, 2005.
- [7] Salvator Roberto Amendolia, Waseem Hassan, Tamas Hauer, David Manset, Richard McClatchey, Dmitry Rogulin , and Tony Solomonides. MammoGrid: a service oriented architecture based medical grid application. In *Grid and Cooperative Computing-GCC 2004*, pages 939–942. Springer, 2004.
- [8] Kevin A Archie and Daniel S Marcus. DicomBrowser: software for viewing and modifying DICOM metadata. *Journal of digital imaging*, 25(5):635–645, 2012.
- [9] Chloé Audigier, Tommaso Mansi, Hervé Delingette, Saikiran Rapaka, Viorel Mihalef, Daniel Carnegie, Emad Boctor, Michael Choti, Ali Kamen, Nicholas Ayache et al. Efficient Lattice Boltzmann Solver for Patient-Specific Radiofrequency Ablation of Hepatic Tumors. *Medical Imaging, IEEE Transactions on*, 34(7):1576–1589, 2015.
- [10] Dirk Bartz, Dirk Mayer, Jan Fischer, Sebastian Ley, Anxo del Rio, Steffi Thust, Claus Peter Heussel, Hans-Ulrich Kauczor , and Wolfgang Straßer. Hybrid segmentation and exploration of the human lungs. In *Visualization, 2003. VIS 2003. IEEE*, pages 177–184. IEEE, 2003.
- [11] Christos Bellos, Athanasios Bibas, Dimitrios Kikidis, Stella Elliott, Stefan Stenfelt, Ratnesh Sahay, Konstantina Nikita, Dimitris Koutsouris , and Dimitrios I Fotiadis. SIFEM Project: Semantic Infostructure interlinking an open source Finite Element tool and libraries with a model repository

- for the multi-scale Modelling of the inner-ear. In *Bioinformatics and Bioengineering (BIBE), 2013 IEEE 13th International Conference on*, pages 1–4. IEEE, 2013.
- [12] Siegfried Benkner, Chris Borckholder, Marian Bubak, Yuriy Kaniovskiy, Richard Knight, Martin Koehler, Spiros Koulouzis, Piotr Nowakowski, and Samuel Wood. A Cloud-based framework for collaborative data management in the VPH-Share Project. In *Advanced Information Networking and Applications Workshops (WAINA), 2013 27th International Conference on*, pages 1203–1210. IEEE, 2013.
- [13] Siegfried Benkner, G Englebrecht, GW Backfrieder, Guntram Berti, Jochen Fingberg, Greg Kohring, JG Schmidt, Stuart E Middleton, D Jones, and J Fenner. Numerical simulation for ehealth: Grid-enabled medical simulation services. 2003.
- [14] Guntram Berti, S Benker, John W Fenner, Jochen Fingberg, Guy Lonsdale, Stuart E Middleton, and Mike Surridge. Medical simulation services via the grid. 2003.
- [15] Marian Bubak, Marek Kasztelnik, Maciej Malawski, Jan Meizner, Piotr Nowakowski, and Sumir Varma. Evaluation of cloud providers for VPH applications. In *Cluster, Cloud and Grid Computing (CCGrid), 2013 13th IEEE/ACM International Symposium on*, pages 200–201. IEEE, 2013.
- [16] KS Burrowes, J De Backer, R Smallwood, PJ Sterk, I Gut, R Wirix-Speetjens, S Siddiqui, J Owers-Bradley, J Wild, D Maier et al. Multi-scale computational models of the airways to unravel the pathophysiological mechanisms in asthma and chronic obstructive pulmonary disease (Air-PROM). *Interface focus*, 3(2):20120057, 2013.
- [17] Eryk Ciepiela, Joanna Kocot, Tomasz Gubala, Maciej Malawski, Marek Kasztelnik, Marian Bubak et al. Gridspace engine of the virolab virtual laboratory. 2008.
- [18] A Crozier, CM Augustin, A Neic, AJ Prassl, M Holler, TE Fastl, A Henemuth, K Bredies, T Kuehne, MJ Bishop et al. Image-based personalization of cardiac anatomy for coupled electromechanical modeling. *Annals of biomedical engineering*, 44(1):58–70, 2016.
- [19] Vasa Curcin and Moustafa Ghanem. Scientific workflow systems-can one size fit all? In *Biomedical Engineering Conference, 2008. CIBEC 2008. Cairo International*, pages 1–9. IEEE, 2008.
- [20] Sandra L de Montbrun and Helen MacRae. Simulation in surgical education. *Clinics in colon and rectal surgery*, 25(3):156, 2012.
- [21] Gerhard Engelbrecht and Siegfried Benkner. A service-oriented Grid environment with on-demand QoS support. In *Services-I, 2009 World Conference on*, pages 147–150. IEEE, 2009.

- [22] Jochen Fingberg, Guntram Berti, Ulrich Hartmann, Achim Basermann, Falk Zimmermann, C Wolters, Alfred Anwander, Avril McCarthy , and Steve Woods. Bio-numerical simulations with SimBio. *NEC Research and Development*, 44(1):140–145, 2003.
- [23] Joerg Freund, Dorin Comaniciu, Yannis Ioannis, Peiya Liu, Richard McClatchey, Edwin Morley-Fletcher, Xavier Pennec, Giacomo Pongiglione , and X Zhou. Health-e-child: an integrated biomedical platform for grid-based paediatric applications. *Studies in health technology and informatics*, 120:259, 2006.
- [24] Paulo A Garcia, Rafael V Davalos , and Damijan Miklavcic. A numerical investigation of the electric and thermal cell kill distributions in electroporation-based therapies in tissue. *PloS one*, 9(8):0, 2014.
- [25] John Geddes, Sharon Lloyd, Andrew Simpson, Martin Rossor, Nick Fox, Derek Hill, Joseph Hajnal, S Lawrie, A McIntosh, E Johnstone et al. NeuroGrid: “Collaborative Neuroscience via Grid Computing”. In *Proceedings All Hands Meeting 2005*. 2004.
- [26] Jeremy Goecks, Anton Nekrutenko, James Taylor et al. Galaxy: a comprehensive approach for supporting accessible, reproducible, and transparent computational research in the life sciences. *Genome Biol*, 11(8):0, 2010.
- [27] Andy Haines, Shyama Kuruville , and Matthias Borchert. Bridging the implementation gap between knowledge and action for health. *Bulletin of the World Health Organization*, 82(10):724–731, 2004.
- [28] Niobe Haitas and T Glatard. Distributed computing for neurosciences: the N4U example. *Journées Scientifiques Mésocentres et France Grilles*, 2012.
- [29] Sheldon K Hall, Ean H Ooi , and Stephen J Payne. Cell death, perfusion and electrical parameters are critical in models of hepatic radiofrequency ablation. *International Journal of Hyperthermia*, (in press):1–13, 2015.
- [30] Mark Hartswood, Marina Jirotko, Rob Procter, Roger Slack, Alex Voss , and Sharon Lloyd. Working IT out in e-Science: Experiences of requirements capture in a HealthGrid project. *Studies in health technology and informatics*, 112:198–209, 2005.
- [31] P Hildebrand, T Leibecke, M Kleemann, L Mirow, M Birth, HP Bruch , and C Bürk. Influence of operator experience in radiofrequency ablation of malignant liver tumours on treatment outcome. *European Journal of Surgical Oncology (EJSO)*, 32(4):430–434, 2006.
- [32] Duncan Hull, Katy Wolstencroft, Robert Stevens, Carole Goble, Mathew R Pocock, Peter Li , and Tom Oinn. Taverna: a tool for building and running workflows of services. *Nucleic acids research*, 34(suppl 2):0, 2006.

- [33] Razvan Ioan Ionasec, Ingmar Voigt, Bogdan Georgescu, Yang Wang, Helene Houle, Fernando Vega-Higuera, Nassir Navab , and Dorin Comaniciu. Patient-specific modeling and quantification of the aortic and mitral valves from 4-D cardiac CT and TEE. *Medical Imaging, IEEE Transactions on*, 29(9):1636–1651, 2010.
- [34] Hrvoje Jasak, Aleksandar Jemcov , and Zeljko Tukovic. OpenFOAM: A C++ library for complex physics simulations. In *International workshop on coupled methods in numerical dynamics*, volume 1000, pages 1–20. 2007.
- [35] David Johnson, Steve McKeever, Thomas S Deisboeck , and Zhihui Wang. Connecting digital cancer model repositories with markup: introducing TumorML version 1.0. *ACM SIGBioinformatics Record*, 3(3):5–11, 2013.
- [36] David Johnson, Steve McKeever, Georgios Stamatakos, Dimitra Dionysiou, Norbert Graf, Vangelis Sakkalis, Konstantinos Marias, Zhihui Wang , and Thomas S Deisboeck. Dealing with diversity in computational cancer modeling. *Cancer informatics*, 12:115, 2013.
- [37] Özgür Kafalı, Stefano Bromuri, Michal Sindlar, Tom van der Weide, Eduardo Aguilar Pelaez, Ulrich Schaechtle, Bruno Alves, Damien Zufferey, Esther Rodriguez-Villegas, Michael Ignaz Schumacher et al. COMMODITY12: A smart e-health environment for diabetes management. *Journal of Ambient Intelligence and Smart Environments*, 5(5):479–502, 2013.
- [38] Bernhard Kerbl, Philip Voglreiter, Rostislav Khlebnikov, Dieter Schmalstieg, Daniel Seider, Michael Moche, Philipp Stiegler, Rupert H Portugaller , and Bernhard Kainz. Intervention Planning of Hepatocellular Carcinoma Radio-Frequency Ablations. In *Clinical Image-Based Procedures. From Planning to Intervention*, pages 9–16. Springer, 2012.
- [39] Bernhard Kerbl, Philip Voglreiter, Rostislav Khlebnikov, Dieter Schmalstieg, Daniel Seider, Michael Moche, Philipp Stiegler, Rupert H Portugaller , and Bernhard Kainz. Intervention Planning of Hepatocellular Carcinoma Radio-Frequency Ablations. In *Clinical Image-Based Procedures. From Planning to Intervention*, pages 9–16. Springer, 2013.
- [40] Rostislav Khlebnikov, Philip Voglreiter, Markus Steinberger, Bernhard Kainz , and Dieter Schmalstieg. Parallel Irradiance Caching for Interactive Monte-Carlo Direct Volume Rendering. In *Computer Graphics Forum*, volume 33, pages 61–70. Wiley Online Library, 2014.
- [41] Arno Klein, Jesper Andersson, Babak A Ardekani, John Ashburner, Brian Avants, Ming-Chang Chiang, Gary E Christensen, D Louis Collins, James Gee, Pierre Hellier et al. Evaluation of 14 nonlinear deformation algorithms applied to human brain MRI registration. *Neuroimage*, 46(3):786–802, 2009.

- [42] Andrzej A Kononowicz, Andrew J Narracott, Simone Manini, Martin J Bayley, Patricia V Lawford, Keith McCormack , and Nabil Zary. A framework for different levels of integration of computational models into web-based virtual patients. *Journal of medical Internet research*, 16(1):0, 2014.
- [43] Spiros Koulouzis, Dmitry Vasyunin, Reginald Cushing, Adam Belloum , and Marian Bubak. Cloud data federation for scientific applications. In *Euro-Par 2013: Parallel Processing Workshops*, pages 13–22. Springer, 2013.
- [44] Vadym Kramar, Minna Korhonen , and Yury Sergeev. Particularities of visualisation of medical and wellness data through a digital patient avatar. In *Open Innovations Association (FRUCT), 2013 14th Conference of*, pages 45–56. IEEE, 2013.
- [45] Thomas M Krummel. Surgical simulation and virtual reality: the coming revolution. *Annals of surgery*, 228(5):635, 1998.
- [46] Tim Kröger, Inga Altrogge, Tobias Preusser, Philippe L Pereira, Diethard Schmidt, Andreas Weihusen , and Heinz-Otto Peitgen. Numerical simulation of radio frequency ablation with state dependent material parameters in three space dimensions. In *Medical Image Computing and Computer-Assisted Intervention–MICCAI 2006*, pages 380–388. Springer, 2006.
- [47] Ignacio Larrabide, Pedro Omedas, Yves Martelli, Xavier Planes, Maarten Nieber, Juan A Moya, Constantine Butakoff, Rafael Sebastián, Oscar Camara, Mathieu De Craene et al. GIMIAS: an open source framework for efficient development of research tools and clinical prototypes. In *Functional Imaging and Modeling of the Heart*, pages 417–426. Springer, 2009.
- [48] Marc Levoy. Efficient ray tracing of volume data. *ACM Transactions on Graphics (TOG)*, 9(3):245–261, 1990.
- [49] Anders Logg, Kent-Andre Mardal, Garth N. Wells et al. *Automated Solution of Differential Equations by the Finite Element Method*. Springer, 2012.
- [50] Steve McKeever and David Johnson. The role of markup for enabling interoperability in health informatics. *Frontiers in physiology*, 6, 2015.
- [51] Viorel Mihalef, Razvan Ioan Ionasec, Puneet Sharma, Bogdan Georgescu, Ingmar Voigt, Michael Suehling , and Dorin Comaniciu. Patient-specific modelling of whole heart anatomy, dynamics and haemodynamics from four-dimensional cardiac CT images. *Interface Focus*, 1(3):286–296, 2011.
- [52] Hoang Anh Nguyen, David Abramson, Timoleon Kipouros, Andrew Janke , and Graham Galloway. WorkWays: interacting with scientific workflows. *Concurrency and Computation: Practice and Experience*, 27(16):4377–4397, 2015.

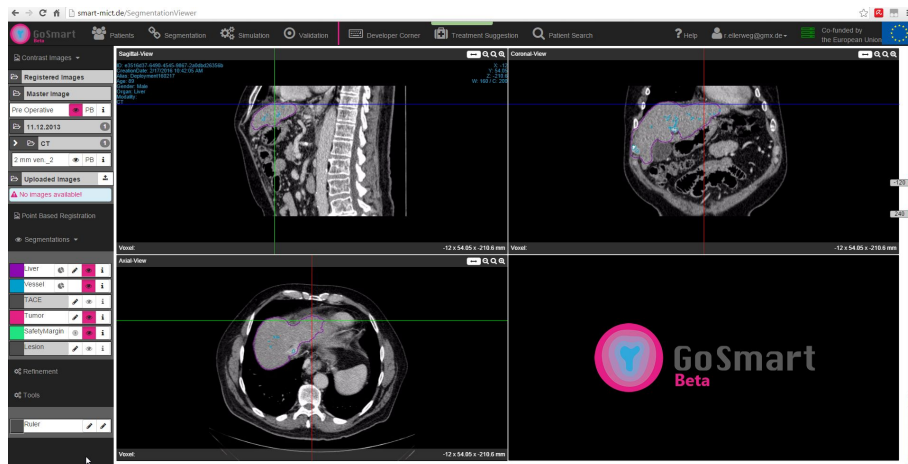
- [53] David P O’Neill, Tingying Peng, Philipp Stiegler, Ursula Mayrhauser, Sonja Koestenbauer, Karlheinz Tscheliessnigg , and Stephen J Payne. A three-state mathematical model of hyperthermic cell death. *Ann. Biomed. Eng.*, 39(1):570–579, 2011.
- [54] Tom Oinn, Mark Greenwood, Matthew Addis, M Nedim Alpdemir, Justin Ferris, Kevin Glover, Carole Goble, Antoon Goderis, Duncan Hull, Darren Marvin et al. Taverna: lessons in creating a workflow environment for the life sciences. *Concurrency and Computation: Practice and Experience*, 18(10):1067–1100, 2006.
- [55] Francesco Pappalardo, Mark D Halling-Brown, Nicolas Rapin, Ping Zhang, Davide Alemani, Andrew Emerson, Paola Paci, Patrice Duroux, Marzio Pennisi, Arianna Palladini et al. ImmunoGrid, an integrative environment for large-scale simulation of the immune system for vaccine discovery, design and optimization. *Briefings in Bioinformatics*, 10(3):330–340, 2009.
- [56] Umang Patel, Alberto Marzo, Alan Waterworth, DR Hose, Alejandro Frangi, Pat Lawford, Keith McCormack , and Stuart Coley. Development of a Computational Model to Determine the Risk of Aneurysm Rupture. 2007.
- [57] Stephen Payne, Ronan Flanagan, Mika Pollari, Tuomas Alhonnoro, Claire Bost, David O’Neill, Tingying Peng , and Philipp Stiegler. Image-based multi-scale modelling and validation of radio-frequency ablation in liver tumours. *Phil. Trans. R. Soc. Lond. A*, 369(1954):4233–4254, 2011.
- [58] JMT Penrose, DR Hose, CJ Staples, IS Hamill, IP Jones , and D Sweeney. Fluid structure interactions: coupling of CFD and FE. In *18th CAD-FEM User’s Meeting-International Congress on FEM Technology*. 2000.
- [59] Pablo Perel, Ian Roberts, Emily Sena, Philipa Wheble, Catherine Briscoe, Peter Sandercock, Malcolm Macleod, Luciano E Mignini, Pradeep Jayaram, Khalid S Khan et al. Comparison of treatment effects between animal experiments and clinical trials: systematic review. *Bmj*, 334(7586):197, 2007.
- [60] Gorazd Pucihar, Jasna Krmelj, Matej Rebersek, Tina Batista Napotnik , and Damijan Miklavcic. Equivalent pulse parameters for electroporation. *Biomedical Engineering, IEEE Transactions on*, 58(11):3279–3288, 2011.
- [61] Alberto Redolfi, Richard McClatchey, Ashiq Anjum, Alex Zijdenbos, David Manset, Frederik Barkhof, Christian Spenger, Yannik Legré, Lars-Olof Wahlund, Chiara Barattieri di San Pietro et al. Grid infrastructures for computational neuroscience: the neuGRID example. *Future Neurology*, 4(6):703–722, 2009.

- [62] Christian Rieder, Thorben Kroeger, Christian Schumann , and Horst K Hahn. GPU-based real-time approximation of the ablation zone for radiofrequency ablation. *Visualization and Computer Graphics, IEEE Transactions on*, 17(12):1812–1821, 2011.
- [63] Simona Rossi, Marie-Luise Christ-Neumann, Stefan Rüping, FM Buffa, Dennis Wegener, G McVie, PV Coveney, N Graf , and M Delorenzi. P-Medicine: from data sharing and integration via VPH models to personalized medicine. *Ecancermedicalscience*, 5(1, article 218), 2011.
- [64] Juha Ruokolainen. *Elmer MATC Manual*.
- [65] Asbjørn Rygg, Paul Roe, On Wong , and Jiro Sumitomo. GPFlow: an intuitive environment for web-based scientific workflow. *Concurrency and Computation: Practice and Experience*, 20(4):393–408, 2008.
- [66] Peter Råback and Mika Malinen. Overview of Elmer. 2015.
- [67] Vangelis Sakkalis, Stelios Sfakianakis , and Kostas Marias. Bridging Social Media Technologies and Scientific Research: A Twitter-Enabled Platform for VPH Modeling. In *Wireless Mobile Communication and Healthcare*, pages 380–387. Springer, 2012.
- [68] Vangelis Sakkalis, Stelios Sfakianakis, Eleftheria Tzamali, Kostas Marias, Georgios Stamatakos, Fay Misichroni, Eleftherios Ouzounoglou, Eleni Kolokotroni, Dimitra Dionysiou, David Johnson et al. Web-based workflow planning platform supporting the design and execution of complex multi-scale cancer models. *Biomedical and Health Informatics, IEEE Journal of*, 18(3):824–831, 2014.
- [69] Dick Sawyer. Do it by Design. *An introduction to human factors in medical devices*. Rockville: US Department of Health and Human Services, 1996.
- [70] Tarek Sherif, Pierre Rioux, Marc-Etienne Rousseau, Nicolas Kassis, Nat-acha Beck, Reza Adalat, Samir Das, Tristan Glatard , and Alan C Evans. CBRAIN: a web-based, distributed computing platform for collaborative neuroimaging research. *Recent Advances and the Future Generation of Neuroinformatics Infrastructure*, page 102, 2015.
- [71] Michael A Sherman, Jack L Middleton, Jeanette P Schmidt, David S Paik, Silvia S Blemker, Ayman W Habib, Frank C Anderson, Scott L Delp , and Russ B Altman. The SimTK framework for physics-based simulation of biological structures: preliminary design. In *Proceedings of the Workshop on Component Models and Frameworks in High Performance Computing*. 2005.
- [72] Andrew Simpson, David Power, Douglas Russell, Mark Slaymaker, Vernon Bailey, Chris Tromans, Michael Brady , and Lionel Tarassenko. GIMI: the past, the present and the future. *Philosophical Transactions of the Royal*

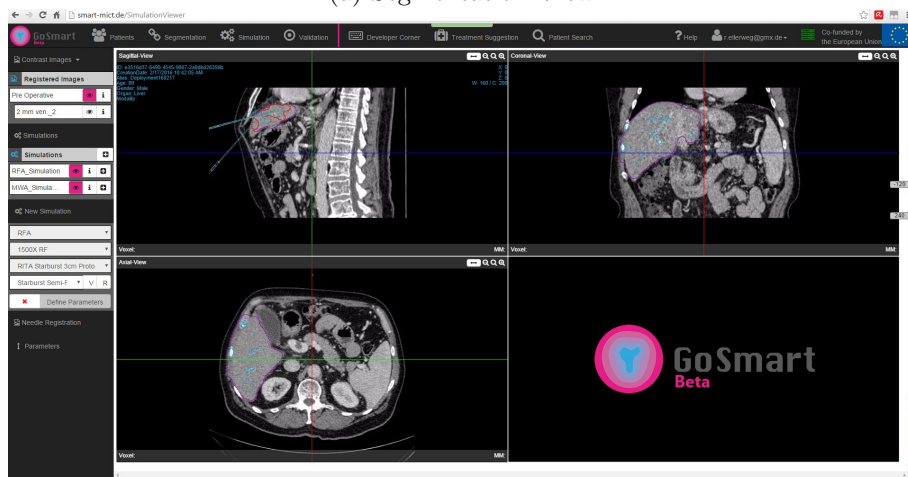
Society of London A: Mathematical, Physical and Engineering Sciences, 368(1925):3891–3905, 2010.

- [73] Nic Smith, Adelaide de Vecchi, Matthew McCormick, David Nordsletten, Oscar Camara, Alejandro F Frangi, Hervé Delingette, Maxime Sermesant, Jatin Relan, Nicholas Ayache et al. EuHeart: personalized and integrated cardiac care using patient-specific cardiovascular modelling. *Interface focus*, page 0, 2011.
- [74] G Stamatakos, Dimitra Dionysiou, Fay Misichroni, Norbert Graf, Stefaan van Gool, Rainar Bohle, Feng Dong, Marco Viceconti, Kostas Marias, Vangelis Sakkalis et al. Computational Horizons In Cancer (CHIC): Developing Meta-and Hyper-Multiscale Models and Repositories for In Silico Oncology—a Brief Technical Outline of the Project. In *6th International Advanced Research Workshop on In Silico Oncology and Cancer Investigation—The CHIC Project Workshop (IARWISOCI)*, page 9. 2014.
- [75] Georgios S Stamatakos, Eleni C Georgiadi, Norbert Graf, Eleni A Kolokotroni, and Dimitra D Dionysiou. Exploiting clinical trial data drastically narrows the window of possible solutions to the problem of clinical adaptation of a multiscale cancer model. *PLoS One*, 6(3):0, 2011.
- [76] NS Sung, WF Crowley Jr, M Genel, and et al. Central challenges facing the national clinical research enterprise. *JAMA*, 289(10):1278–1287, 2003.
- [77] D Tartarini, M Viceconti, N Gruel, K Duan, and DC Walker. The VPH Hypermodelling framework for cancer multiscale models in the clinical practice. In *In Silico Oncology and Cancer Investigation (IARWISOCI), 2014 6th International Advanced Research Workshop on*. Institute of Electrical and Electronics Engineers, 2014.
- [78] Debora Testi, Daniel Harezlak, Ernesto Coto, Juan Arenas, and Vadim Surpin. D6.5: Production Deployment of User Access Systems. Public Deliverable, Virtual Physiological Human: Sharing for Healthcare – A Research Environment (VPH-Share), Feb 2014.
- [79] Rainer Thiel, Marco Viceconti, and Karl A Stroetmann. Assessing bio-computational modelling in transforming clinical guidelines for osteoporosis management. In *MIE*, pages 432–436. 2011.
- [80] Marco Viceconti and Andrew D McCulloch. Policy needs and options for a common approach towards modelling and simulation of human physiology and diseases with a focus on the virtual physiological human. *Studies in health technology and informatics*, 170:49–82, 2011.
- [81] Philip Voglreiter, Markus Steinberger, Rostislav Khlebnikov, Bernhard Kainz, and Dieter Schmalstieg. Volume Rendering with advanced GPU scheduling strategies. 2013.

- [82] Phil Weir, Dominic Reuter, Roland Ellerweg, Tuomas Alhonnoro, Mika Pollari, Philip Voglreiter, Panchatcharam Mariappan, Ronan Flanagan, Chang Sub Park, Stephen Payne et al. Go-Smart: Web-based Computational Modeling of Minimally Invasive Cancer Treatments. 2015.
- [83] Mark D Wilkinson and Matthew Links. BioMOBY: an open source biological web services proposal. *Briefings in bioinformatics*, 3(4):331–341, 2002.



(a) Segmentation View



(b) Simulation Preparation

Figure 3: Screenshots of workflow using in-browser client. Browser used is Google Chrome

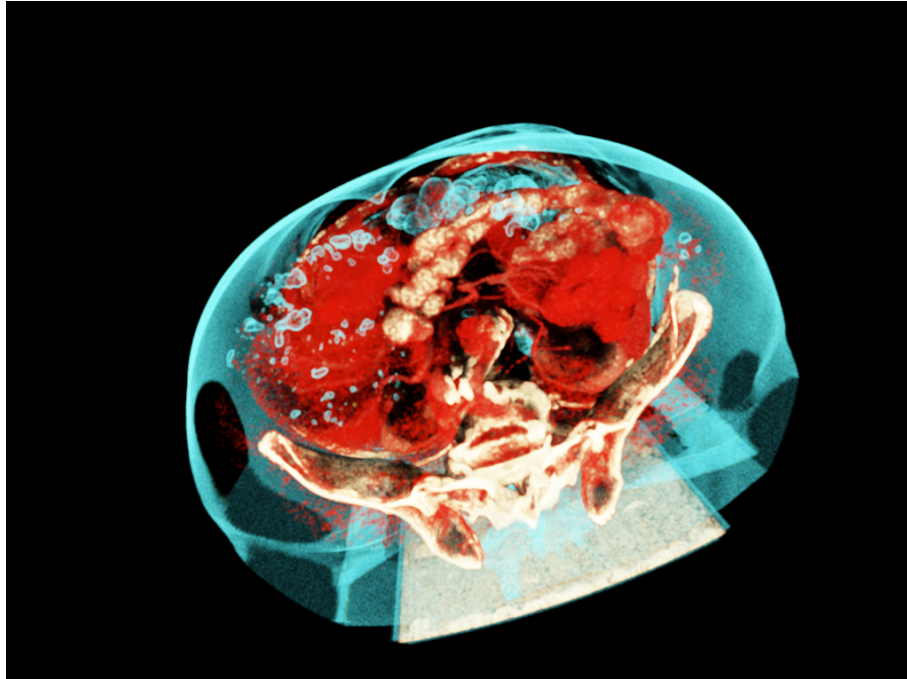


Figure 4: Example output of VisApp renderer on high quality setting

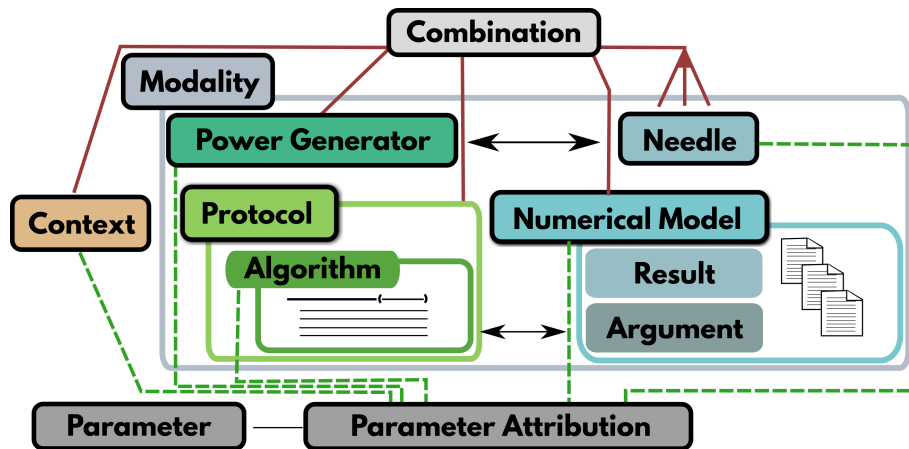


Figure 5: Overview of relationships between fundamental entities. Red solid lines indicate component entities of a combination (needles with multiplicity), green dashed lines indicate parameterizable entities. White lines indicate (usually textual) definitions stored in the persistence layer, that is within the entity's record.

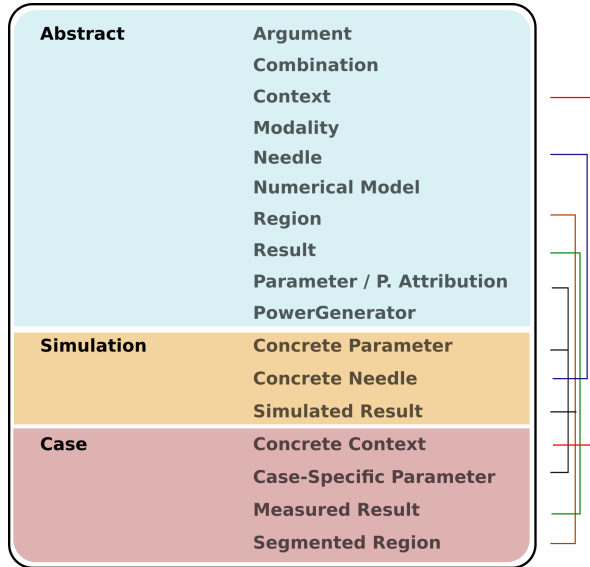


Figure 6: Clinical domain entities arranged in Abstract-Simulation-Case (ASC) tiers. Concretization (or measurement) relationships are indicated by bracket lines on far right.

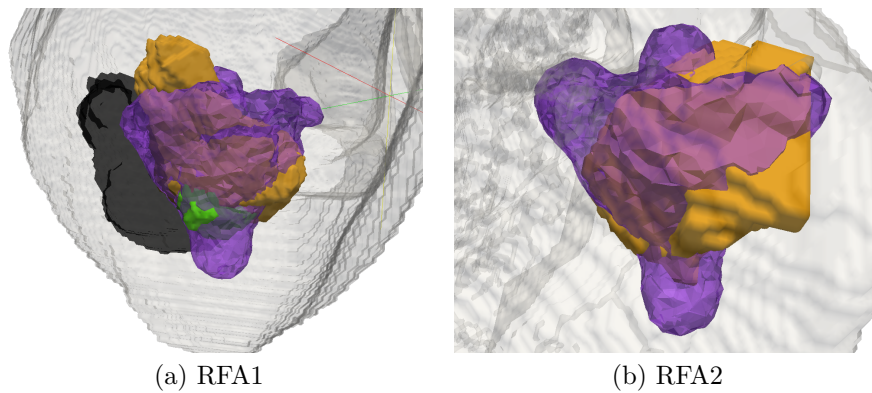
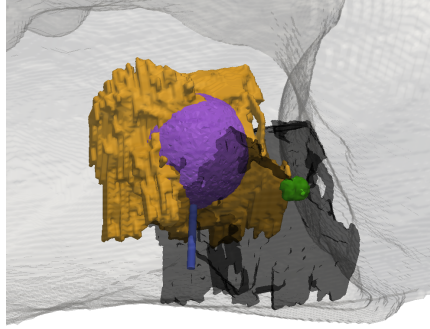
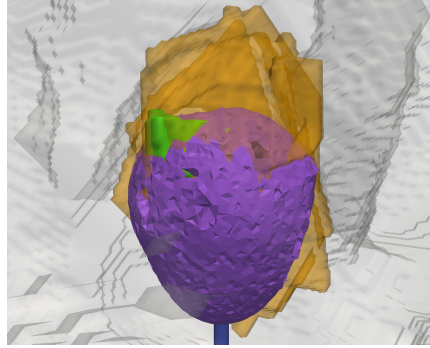


Figure 7: Radiofrequency ablation profiles for two cases. Purple: simulated lesion; orange: simulated lesion; green: tumour [in (a)]; charcoal: segmented lesion before rigid body registration [in (a)]; light-grey outline: organ

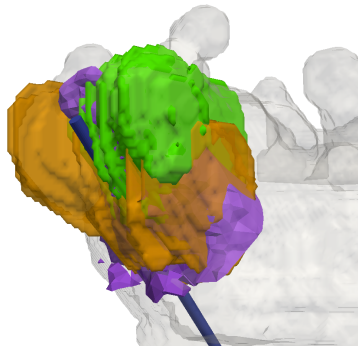


(a) MWA2

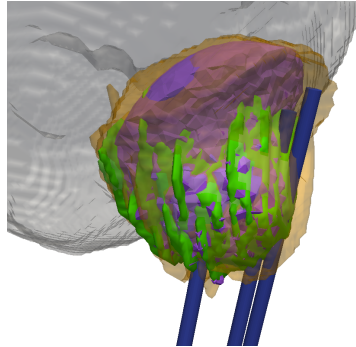


(b) MWA4

Figure 8: Microwave ablation profiles for two cases. Purple: simulated lesion; orange: simulated lesion; green: tumour; charcoal: segmented lesion before rigid body registration [in (a)]; light-grey outline: organ; blue cylinder: ablation needle

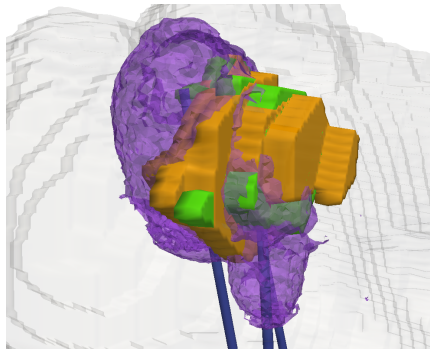


(a) CRYO1

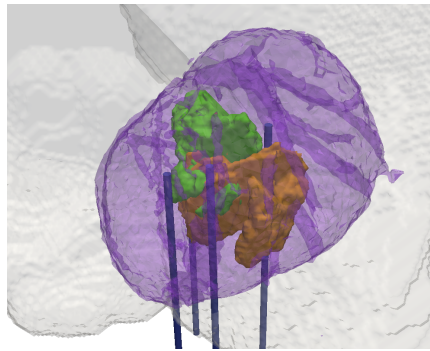


(b) CRYO3

Figure 9: Cryoablation profiles for two cases. Purple: simulated lesion; orange: simulated lesion; green: tumour; light-grey outline: organ; blue cylinder: ablation needle



(a) IRE2



(b) IRE4

Figure 10: Irreversible electroporation profiles for two cases. Purple: simulated lesion; orange: simulated lesion; green: tumour; light-grey outline: organ; blue cylinder: ablation needle